The First Determination of the Energy Difference between Solid-State Conformers by X-ray Diffraction: 1. The Crystal Structure of the Pseudo-Jahn–Teller Complex (Nitrito)bis(2,2′-bipyridyl)copper(II) Nitrate at 20, 100, 165, and 296 K and of Its Isostructural Zinc(II) Analogue at 295 K. 2. The Possibility of Using X-ray Diffraction to Characterize Adiabatic Potential Energy Surfaces and Relative Ligand Strengths

Charles J. Simmons,*[1a] Brian J. Hathaway,[1b] Kitti Amornjarusiri,[1b] Bernard D. Santarsiero,[1c] and Abraham Clearfield[1d]

Contribution from the Department of Chemistry, University of Puerto Rico, Rio Piedras, Puerto Rico 00931. *Received August 20, 1986*

Abstract: The first determination of the energy difference (ΔE) between solid-state conformers by X-ray diffraction is reported for the pseudo-Jahn–Teller complex $[Cu(bpy)_2(ONO)]NO_3$; X-ray data were collected at 20, 100, 165, and 296 K. By invoking an adiabatic potential energy surface consisting of two nonequivalent ground-state minima and by applying Boltzmann statistics to it, ΔE could be determined (77 cm^{-1}) from the temperature variation of the structure of the CuN_4O_2 chromophore. The crystal structure of the isostructural and orbitally nondegenerate $[Zn(bpy)_2(ONO)]NO_3$ complex was also determined, at 295 K. Both complexes crystallize in the monoclinic space group $P2_1/n$ with $Z = 4$. The unit cell parameters are a = 11.067 (2) Å, b = 12.014 (3) Å, c = 14.855 (7) Å, β = 100.01 (3)°, V = 1945 (1) Å^3, d_{calcd} = 1.653 g cm^{-3}, T = 20 K; a = 11.168 (4) Å, b = 11.945 (5) Å, c = 14.909 (6) Å, β = 99.32 (3)°, V = 1962 (1) Å^3, d_{calcd} = 1.638 g cm^{-3}, T = 100 K; a = 11.217 (2) Å, b = 11.936 (5) Å, c = 14.969 (3) Å, β = 99.14 (2)°, V = 1979 (2) Å^3, d_{calcd} = 1.624 g cm^{-3}, T = 165 K; a = 11.225 (2) Å, b = 12.035 (5) Å, c = 15.109 (5) Å, β = 99.55 (2)°, V = 2013 (2) Å^3, d_{calcd} = 1.597 g cm^{-3}, T = 296 K for $[Cu(bpy)_2(ONO)]NO_3$ and a = 11.292 (3) Å, b = 11.962 (4) Å, c = 15.384 (5) Å, β = 101.16 (2)°, V = 2039 (1) Å^3, d_{calcd} = 1.582 g cm^{-3}, T = 295 K for $[Zn(bpy)_2(ONO)]NO_3$. Full-matrix least-squares refinements using 3442 (all data; T = 20 K), 3480 (all data; T = 100 K), 2921 ($I > 2\sigma$; T = 165 K), and 2142 ($I > 2\sigma$; T = 296 K) reflections for $[Cu(bpy)_2(ONO)]NO_3$ and 2185 ($I > 3\sigma$; T = 295 K) for $[Zn(bpy)_2(ONO)]NO_3$ gave the following R_1, R_2, and GOF (goodness-of-fit) values: 0.037, 0.028, 1.44; 0.044, 0.032, 1.39; 0.046, 0.076, 2.35; 0.046, 0.053, 1.30; and 0.036, 0.044, 2.90, respectively. The possibility of using low-temperature X-ray diffraction and ESR spectroscopy to determine the energies of the vibronically coupled ground and first-excited electronic states in [Cu(bpy or phen)$_2$(OXO)]Y complexes and to obtain the relative ligand strengths of various OXO^- groups ($OXO^- = CH_3CO_2^-$, NO_2^-, etc.) is also discussed.

One group of six-coordinate Cu(II) complexes which have been little studied are those which have nondegenerate electronic ground states but are still susceptible to distortions of a vibronic origin. Probably the most interesting of these so-called "pseudo-Jahn–Teller"[2] complexes are those with the formula $[CuL_2(OXO)]Y$, where L is bpy (2,2′-bipyridyl), phen (1,10-phenanthroline), or bipyam (2,2′-bipyridylamine) and OXO^- is a bidentate ligand such as acetate or nitrite. The first determination of a structure of a $[CuL_2(OXO)]Y$ complex was that of $[Cu(bpy)_2(ONO)]NO_3$ done by Procter and Stephens[3] (1969, room temperature, visually estimated intensities). The structure of the $[Cu(bpy)_2(ONO)]^+$ cation was classified as static cis distorted octahedral,[3,4] with one N atom from each bpy ligand axial and the other two N atoms and both nitrito O atoms equatorial (see Figure 1). ESR and polarized single-crystal electronic spectra measured at room temperature seemed to support an underlying static structure.[5] This view was not questioned until the temperature variability of the ESR spectra of Cu(II)-doped $[Zn(bpy)_2(ONO)]NO_3$ suggested a fluxional CuN_4O_2 chromophore.[6] Subsequent low-temperature X-ray results for $[Cu(bpy)_2(ONO)]NO_3$[7-9] (T = 165 K) and $[Cu(phen)_2(CH_3CO_2)]ClO_4$[10] ($T$ = 173 K) revealed significant changes in the copper(II)–ligand bond lengths, proving that the CuN_4O_2 chromophore is fluxional and that the purported cis octahedral stereochemistry is but one of an increasing number of "pseudo" or "fluxional" coordination geometries being identified for various Cu(II) complexes.[11-15]

At temperatures below 165 K, it is found that the copper-

(1) (a) Department of Chemistry, University of Puerto Rico, Rio Piedras, Puerto Rico 00931. (b) Department of Chemistry, University College, Cork, Ireland. (c) Arthur Amos Noyes Laboratory of Chemical Physics, California Institute of Technology, Pasadena, CA 91125, contribution number 7438. (d) Department of Chemistry, Texas A&M University, College Station, TX 77843.

(2) In accordance with the recommendation recently made by Professor R. Pearson at the VIII Symposium on the Jahn–Teller effect, Marburg, Germany, the term "pseudo-Jahn–Teller" will refer only to the vibronic coupling of nondegenerate electronic states originating from the *same* electronic configuration. It was further recommended that the term "second-order Jahn–Teller" refer only to vibronic coupling involving *different* electronic configurations.

(3) Procter, I. M.; Stephens, F. S. *J. Chem. Soc. A* **1969**, 1248.

(4) Hathaway, B. J.; Billing, D. E. *Coord. Chem. Rev.* **1970**, *5*, 143.

(5) Procter, I. M.; Hathaway, B. J.; Billing, D. E.; Dudley, R.; Nicholls, P. *J. Chem. Soc. A* **1969**, 1192.

(6) Fitzgerald, W.; Murphy, B.; Tyagi, S.; Walsh, B.; Walsh, A.; Hathaway, B. J. *J. Chem. Soc., Dalton Trans.* **1981**, 2271.

(7) Simmons, C. J.; Clearfield, A.; Fitzgerald, W.; Tyagi, S.; Hathaway, B. J. *Inorg. Chem.* **1983**, *22*, 2463.

(8) Simmons, C. J.; Clearfield, A.; Fitzgerald, W.; Tyagi, S.; Hathaway, B. J. *Trans. Am. Cryst. Assoc.* **1984**, *20*, 155.

(9) Simmons, C. J.; Clearfield, A.; Fitzgerald, W.; Tyagi, S.; Hathaway, B. J. *J. Chem. Soc., Chem. Commun.* **1983**, 189.

(10) Simmons, C. J.; Alcock, N. W.; Seff, K.; Fitzgerald, W.; Hathaway, B. J. *Acta Crystallogr., Sect. B: Struct. Crystallogr. Cryst. Chem.* **1985**, *B41*, 42.

(11) Hathaway, B. J. *Coord. Chem. Rev.* **1981**, *35*, 211.

(12) Hathaway, B. J.; Duggan, M.; Murphy, A.; Mullane, J.; Power, C.; Walsh, A.; Walsh, B. *Coord. Chem. Rev.* **1981**, *36*, 267.

(13) Hathaway, B. J. *Coord. Chem. Rev.* **1982**, *41*, 423.

(14) Hathaway, B. J. *Coord. Chem. Rev.* **1983**, *52*, 87.

(15) Hathaway, B. J. *Struct. Bonding* **1984**, *57*, 55.

0002-7863/87/1509-1947$01.50/0

Table I. Experimental Details of the X-ray Diffraction Study of $[Cu(bpy)_2(ONO)]NO_3$ and $[Zn(bpy)_2(ONO)]NO_3$

T, K	20[a]	100[a]	165[a]	296[a]	295[b]
A. Crystal Parameters					
space group	$P2_1/n$	$P2_1/n$	$P2_1/n$	$P2_1/n$	$P2_1/n$
a, Å	11.067 (2)[c]	11.168 (4)[c]	11.217 (2)[d]	11.225 (2)[d]	11.292 (3)[c]
b, Å	12.014 (3)	11.945 (5)	11.936 (5)	12.035 (5)	11.962 (4)
c, Å	14.855 (7)	14.909 (6)	14.969 (3)	15.109 (5)	15.384 (5)
β, deg	100.01 (3)	99.32 (3)	99.14 (2)	99.55 (2)	101.16 (2)
V, Å^3	1945 (1)	1962 (1)	1979 (2)	2013 (2)	2039 (1)
Z	4	4	4	4	4
d_{calcd}, g cm^{-3}	1.653	1.638	1.624	1.597	1.582
μ, cm^{-1} (Mo Kα)	11.5	11.5	11.5	11.5	12.8
B. Data Acquisition Parameters					
cryst size, mm	0.30 × 0.30 × 0.20		0.23 × 0.17 × 0.14		sphere, r = 0.38
diffractometer	modified Syntex $P\bar{1}$		Enraf-Nonius CAD4		Syntex $P1$
radiation	Mo Kα	Mo Kα	Mo Kα	Mo Kα	Mo Kα
scan mode	θ–2θ	θ–2θ	θ–2θ	θ–2θ	θ–2θ
scan speed, deg min^{-1}	3	3	variable[e]	variable[e]	3
bkgrd time/scan time	0.5	0.5	0.5	0.5	0.6
2θ scan width below and above $K\alpha_1$–$K\alpha_2$ angles	0.8	0.8	0.7	0.7	1.0
2θ scan range, deg	3–50	3–50	0–50	0–50	3–45
no. of unique reflcns measd	3442	3480	3477	3535	2678
C. Structure Determination Parameters[f]					
no. reflcns used in least-squares	3442 (all)	3480 (all)	2921 (2σ)	2142 (2σ)	2185 (3σ)
R_1[g]	0.037	0.044	0.046	0.046	0.036
R_2[h]	0.028	0.032	0.076	0.053	0.044
S[i]	1.44	1.39	2.35	1.30	2.90
g(×10^6)[j]	0.54 (4)	0.56 (4)			
largest shift/esd	10%	10%	78%	26%	84%

[a] $[Cu(bpy)_2(ONO)]NO_3$. [b] $[Zn(bpy)_2(ONO)]NO_3$. [c,d] Unit cell constants and their esd's determined by least-squares treatments of the angular coordinates of 15 and 25 high-angle reflections, respectively. [e] All intensities were prescanned at a rate of 20.12° min^{-1} (NPIPRE = 1): those obeying the prescan acceptance limit (SIGMA) of $[\sigma(I)/I]_{pre} < 0.02$ were considered observed and not rescanned, while those obeying the prescan rejection limit (SIGPRE) of $[\sigma(I)/I]_{pre} > 2.0$ were considered unobserved and also not rescanned. All others were rescanned by using variable rates (2.01–20.12° in ω) so that the maximum scan times would not exceed 27 s (165 K) and 31 s (296 K). [f] Calculations were carried out by using the CRYM crystallographic computing package (20 and 100 K data), the Enraf-Nonius structure determination package (165 and 296 K data), and the crystallographic program library of Professor K. Seff, University of Hawaii (295 K data). The weighting schemes used and the functions minimized in the least-squares refinements were as follows: $w = [\sigma(F_o^2)]^{-2}$ (20 and 100 K data), $w = [\sigma(F_o)]^{-2}$ (165, 296, and 295 K data) and $\sum w(F_o^2-F_c^2)^2$ (20 and 100 K data), $\sum w(F_o - F_c)^2$ (165, 296, and 295 K data). [g] $R_1 = \sum||F_o| - |F_c||/\sum F_o$. [h] $R_2 = [\sum w(F_o^2 - F_c^2)^2/\sum wF_o^4]^{1/2}$ (20 and 100 K data) and $R_2 = [\sum w(F_o - |F_c|)^2/wF_o^2]^{1/2}$ (165, 296, and 295 K data). [i] $S = [\sum w(F_o^2 - F_c^2)^2/(n-p)]^{1/2}$ (20 and 100 K data) and $S = [\sum w(F_o - |F_c|)^2/(n-p)]^{1/2}$ (165, 296, and 295 K data), where n = number of observations and p = number of variables (353). [j] g = correction factor for isotropic secondary extinction.

(II)–ligand bond lengths in $[Cu(bpy)_2(ONO)]NO_3$ continue to change and that there is a discernible pattern to this change. An adiabatic potential energy surface consisting of two nonequivalent ground-state minima separated in energy by ΔE is used to rationalize these changes. By assuming Boltzmann statistics and using the metrical data from the structures of the CuN_4O_2 chromophore at various temperatures (here 20, 100, 165, and 296 K), the value of ΔE can be determined. We also discuss the possibility of using X-ray diffraction to further characterize the adiabatic energy surfaces and the relative ligand strengths of the OXO^- groups in the $[CuL_2(OXO)]Y$ complexes. X-ray diffraction has been used to infer chemical reaction pathways from the structural changes that occur in certain chemical groups when they are in different crystalline environments at the same temperature.[16-27] However, it has never before been used to obtain thermodynamic information, such as the energy difference (ΔE) between solid-state conformers, from the structural changes that occur in certain groups when they are in the same crystalline environment but at different temperatures.

Experimental Section

The synthesis of $[Cu(bpy)_2(ONO)]NO_3$ and its Zn(II) analogue have already been reported.[5,28]

X-ray Data Collection. Diffraction intensities for $[Cu(bpy)_2(ONO)]NO_3$ were measured at 20 (±0.5) and 100 (±0.5) K with a modified Syntex $P\bar{1}$ diffractometer equipped with a cryocooler for work at very low temperature[29] and at 165 (±5) and 296 (±1) K with an Enraf-Nonius CAD 4 diffractometer equipped with a concentric stream low-temperature device.[30] Those for $[Zn(bpy)_2(ONO)]NO_3$ were obtained at 295 (±1) K with a Syntex $P\bar{1}$ diffractometer. The intensities of three standard reflections, measured after every 100 reflections (after every 2200 and 4000 s for the 165 and 296 K data), indicated no crystal decomposition during data collection, except for a 3.8 and a 6.5% decay in the 20 and 165 K data, which were subsequently adjusted by assuming a linear decrease in intensity with exposure time. The variance of the net intensities was defined as $\sigma^2(I_0) = [C + (t_c/t_b)^2B]\omega^2 + (pI)^2$, where C is the total integrated count, t_c/t_b the ratio of the total scan time to total background time (e.g., 2 for a CAD 4 diffractometer), B the total background counts, ω the relative scan speed (to 1 deg min^{-1}), and p (0.02 for 20, 100, and 295 K data, 0.05 for 165 and 296 K data) a factor used to downweight intense reflections; $I_0 = \omega[C - (t_c/t_b)B]$. Intensities were not corrected for absorption. The unit cell constants and data acquisition procedures are summarized in Table I.

Structure Refinements. Atomic coordinates from the original room temperature structures of $[Cu(bpy)_2(ONO)]NO_3$[3] and $[Zn(bpy)_2$-

(16) Bürgi, H. B. *Inorg. Chem.* **1973**, *12*, 2321.
(17) Bürgi, H. B.; Dunitz, J. D.; Shefter, E. *J. Am. Chem. Soc.* **1973**, *95*, 5065.
(18) Bürgi, H. B.; Dunitz, J. D.; Shefter, E. *Acta Crystallogr., Sect. B: Struct. Crystallogr. Cryst. Chem.* **1974**, *B30*, 1517.
(19) Bürgi, H. B.; Dunitz, J. D.; Lehn, J. M.; Wipff, G. *Tetrahedron* **1974**, *30*, 1563.
(20) Murray-Rust, P.; Bürgi, H. B.; Dunitz, J. D. *J. Am. Chem. Soc.* **1975**, *97*, 921.
(21) Bürgi, H. B. *Angew. Chem., Int. Ed. Engl.* **1975**, *14*, 460.
(22) Bürgi, H. B.; Shefter, E.; Dunitz, J. D. *Tetrahedron* **1975**, *31*, 3089.
(23) Dunitz, J. D. *X-ray Analysis and the Structure of Organic Molecules*; Cornell University Press: Ithaca, New York, 1979; Chapter 7.
(24) Britton, D.; Dunitz, J. D. *J. Am. Chem. Soc.* **1981**, *103*, 2971.
(25) Bye, E.; Schweizer, W. B.; Dunitz, J. D. *J. Am. Chem. Soc.* **1982**, *104*, 5893.
(26) Bürgi, H. B.; Dunitz, J. D. *Acc. Chem. Res.* **1983**, *16*, 153.
(27) Auf der Hede, T. P. E.; Nassimbeni, L. R. *Inorg. Chem.* **1984**, *23*, 4525.
(28) Walsh, A.; Walsh, B.; Murphy, B.; Hathaway, B. *Acta Crystallogr., Sect. B: Struct. Crystallogr. Cryst. Chem.* **1981**, *B37*, 1512.
(29) Samson, S.; Goldish, E.; Dick, C. J. *J. Appl. Cryst.* **1980**, *13*, 425.
(30) Designed by the Molecular Structure Corporation, College Station, TX.

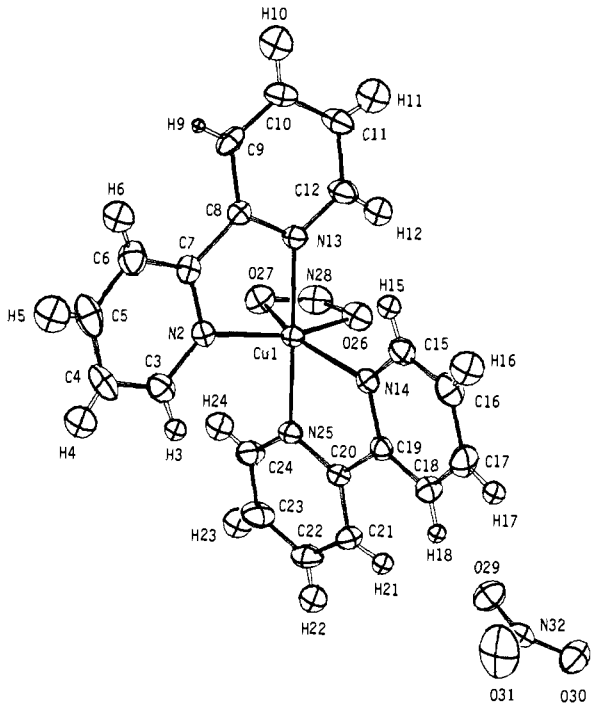

Figure 1. Structure of the pseudo-Jahn–Teller complex, $[Cu(bpy)_2(ONO)]NO_3$, at 296 K; ellipsoids of 25% probability are shown. (Our numbering scheme for the isostructural $[Zn(bpy)_2(ONO)]NO_3$ complex is analogous.) Bonds between M(1) (M = Cu, Zn) and the nearly coplanar N(2), N(14), O(26), and O(27) atoms are "equatorial"; those between M(1) and N(13) and N(25) are "axial".

$(ONO)]NO_3$[28] were used as starting coordinates. The final results (Tables I, II, and III) were obtained by full-matrix least-squares refinements of the 353 parameters, with anisotropic U's for all non-H atoms and isotropic U's for all H atoms. Atomic scattering factors were taken from ref 31a and corrected for anomalous dispersion.[31b]

Results and Discussion

Structural Results for $[Cu(bpy)_2(ONO)]NO_3$ and Its Isostructural Zn(II) Analogue. (See Figure 1). Although the overall structural features of $[Cu(bpy)_2(ONO)]NO_3$ and $[Zn(bpy)_2(ONO)]NO_3$ are similar, especially at room temperature, there are some meaningful differences between them. For example, in the Cu(II) complex the Cu(1)–N(13) and Cu(1)–N(25) axial bonds are significantly shorter (mean = 1.984 (4) Å, T = 296 K) than the Cu(1)–N(2) and Cu(1)–N(14) equatorial bonds (mean = 2.080 (6) Å), whereas in the Zn(II) analogue the Zn-(1)–N_{ax} bonds are longer (mean = 2.130 (4) Å, T = 295 K) than the Zn(1)–N_{eq} bonds (mean = 2.084 (4) Å). Also, the amount of distortion from C_2 symmetry, defined by

$$S = |d_{M_1-O_{27}} - d_{M_1-O_{26}}| + |d_{M_1-N_{14}} - d_{M_1-N_2}| + |d_{M_1-N_{25}} - d_{M_1-N_{13}}| \quad (1)$$

or equivalently

$$S = \Delta d(M - O_{eq}) + \Delta d(M - N_{eq}) + \Delta d(M - N_{ax})$$
$$M = Cu, Zn$$

is much greater in the Cu(II) complex, 0.11 (1) Å, than it is in the Zn(II) complex, 0.03 (1) Å. There are important differences between the Gaussian ellipsoids of the chelating nitrito groups (see Figure 2). Specifically, the principal components of the O atoms ellipsoids in the Cu(II) complex are larger and more anisotropic [rms values, $U_i^{1/2}$ (Å), T = 296 K: O(26) = 0.25, 0.29, 0.35; O(27) = 0.25, 0.28, 0.35] than those in the Zn(II) complex [$U_i^{1/2}$ (Å) values, T = 295 K: O(26) = 0.23, 0.26, 0.29; O(27) = 0.24, 0.25, 0.28]. More importantly, the angles between the major axes (largest U_i) of the O ellipsoids and the M–O bond vectors are 76 and 78° in the Zn(II) complex but only 16 and 24° in the Cu(II) complex, i.e., the major displacements are nearly perpendicular to the Zn–O bonds but approximately parallel to the Cu–O bonds. This preferential "vibration" along a direction nearly parallel to a metal–ligand bond in the Cu compound is contrary to expectations based on bond-stretching and bond-bending energies. Since the crystals of $[Cu(bpy)_2(ONO)]NO_3$ and the Zn(II) analogue are isomorphous, it is reasonable to

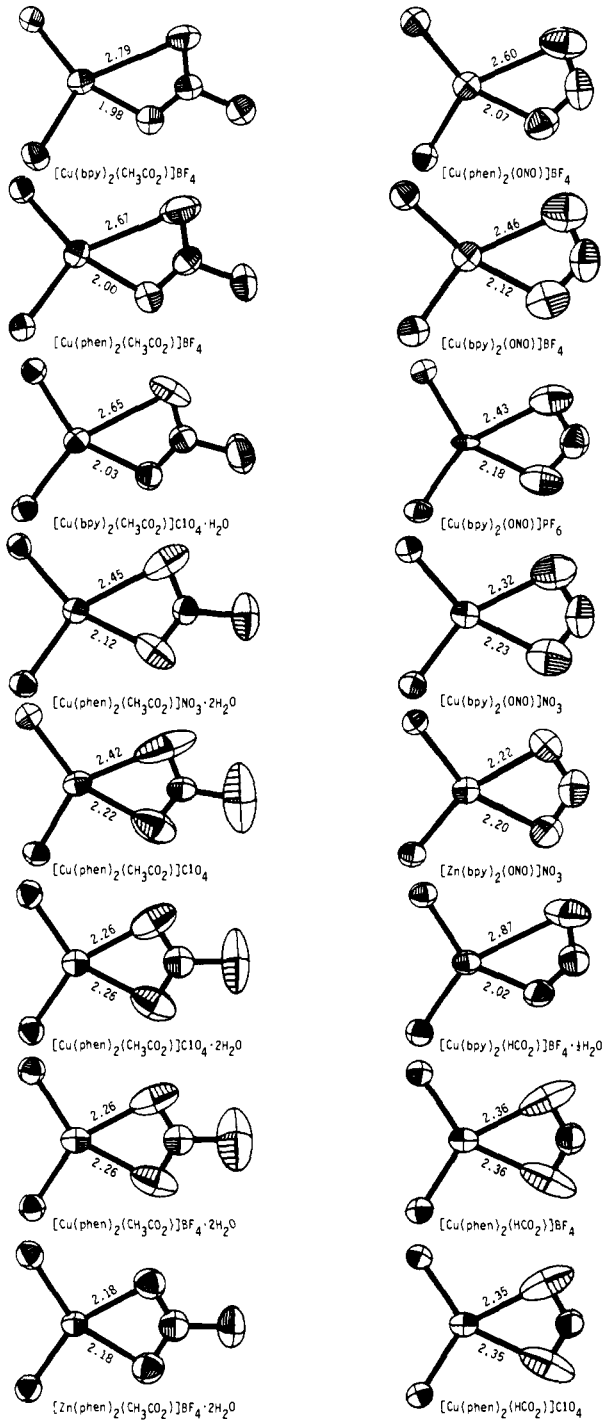

Figure 2. ORTEP drawings (50% probability ellipsoids) of the equatorial atoms in all of the $[ML_2(OXO)]Y$ (M = Cu, Zn) complexes of Table IV. All are drawn to the same scale by using room temperature data; MO_2 groups lie in the plane of the page, and the M–O bond lengths (Å) are indicated. The amplitudes of the acetato O atom Gaussian ellipsoids in $[Cu(phen)_2(CH_3CO_2)]Y\cdot 2H_2O$ (Y = ClO_4 and BF_4) are reduced due to the hydrogen bonding between the O atoms and the water molecules, which are not shown. Note the differences between the ellipsoids of the O atoms in each isomorphous pair of $[M(bpy)_2(ONO)]NO_3$ and $[M-(phen)_2(CH_3CO_2)]BF_4\cdot 2H_2O$ crystals.

(31) (a) *International Tables for X-ray Crystallography*; Kynoch Press: Birmingham, England, 1974; Vol. IV, pp 71–102. (b) International Tables for X-ray Crystallography; Kynoch Press: Birmingham, England, 1974; Vol. IV, p 149.

Table II. Fractional Atomic Coordinates (Non-hydrogen × 10^4, Hydrogen × 10^3)[c]

	T = 20 K[a]			T = 100 K[a]		
	x	y	z	x	y	z
M(1)	2404.6 (3)	467.9 (2)	1213.0 (2)	2401.0 (3)	466.6 (3)	1229.6 (2)
N(2)	3905 (2)	1466 (1)	1371 (1)	3930 (2)	1458 (2)	1384 (1)
C(3)	4385 (2)	2049 (2)	2118 (1)	4427 (2)	2031 (2)	2123 (2)
C(4)	5337 (2)	2794 (2)	2128 (2)	5381 (3)	2758 (2)	2124 (2)
C(5)	5821 (2)	2935 (2)	1335 (2)	5847 (3)	2898 (2)	1328 (2)
C(6)	5342 (2)	2332 (2)	561 (2)	5355 (2)	2304 (2)	561 (2)
C(7)	4387 (2)	1600 (2)	596 (1)	4393 (2)	1587 (2)	604 (2)
C(8)	3772 (2)	928 (2)	−188 (1)	3765 (2)	936 (2)	−176 (2)
C(9)	4193 (2)	851 (2)	−1014 (2)	4179 (2)	848 (2)	−1002 (2)
C(10)	3513 (2)	251 (2)	−1718 (1)	3498 (2)	262 (2)	−1699 (2)
C(11)	2435 (2)	−253 (2)	−1592 (1)	2412 (3)	−213 (2)	−1573 (2)
C(12)	2091 (2)	−181 (2)	−738 (1)	2069 (2)	−132 (2)	−723 (2)
N(13)	2751 (2)	393 (1)	−51 (1)	2738 (2)	428 (2)	−38 (1)
N(14)	971 (2)	1686 (1)	1070 (1)	998 (2)	1667 (2)	1097 (1)
C(15)	567 (2)	2349 (2)	356 (1)	603 (2)	2329 (2)	390 (2)
C(16)	−313 (2)	3163 (2)	384 (2)	−275 (2)	3140 (2)	413 (2)
C(17)	−821 (2)	3271 (2)	1166 (2)	−793 (2)	3245 (2)	1191 (2)
C(18)	−419 (2)	2581 (2)	1905 (2)	−402 (2)	2557 (2)	1925 (2)
C(19)	496 (2)	1805 (2)	1845 (1)	510 (2)	1782 (2)	1867 (2)
C(20)	1066 (2)	1086 (2)	2619 (1)	1065 (2)	1067 (2)	2638 (2)
C(21)	616 (2)	998 (2)	3432 (2)	622 (2)	978 (2)	3446 (2)
C(22)	1250 (2)	362 (2)	4134 (1)	1253 (2)	347 (2)	4142 (2)
C(23)	2322 (2)	−165 (2)	4019 (2)	2305 (3)	−186 (2)	4021 (2)
C(24)	2702 (2)	−76 (2)	3186 (1)	2676 (3)	−107 (2)	3185 (2)
N(25)	2087 (2)	530 (1)	2495 (1)	2074 (2)	503 (2)	2504 (1)
O(26)	1334 (1)	−936 (1)	1042 (1)	1308 (2)	−1029 (2)	1061 (1)
O(27)	3149 (1)	−1521 (1)	1482 (1)	3124 (2)	−1434 (2)	1450 (1)
N(28)	2044 (2)	−1774 (2)	1254 (1)	2076 (2)	−1800 (2)	1260 (1)
O(29)	−2084 (1)	323 (1)	3770 (1)	−2093 (2)	299 (1)	3745 (1)
O(30)	−3886 (1)	1042 (1)	3797 (1)	−3860 (2)	1030 (2)	3812 (1)
O(31)	−2330 (1)	2121 (1)	3689 (1)	−2314 (2)	2102 (2)	3718 (1)
N(32)	−2767 (2)	1168 (2)	3752 (1)	−2760 (2)	1149 (2)	3759 (1)
H(3)	403 (2)	193 (2)	262 (1)	409 (2)	192 (2)	262 (2)
H(4)	563 (2)	315 (2)	267 (1)	572 (2)	308 (2)	265 (2)
H(5)	644 (2)	343 (2)	133 (1)	644 (2)	336 (2)	129 (2)
H(6)	569 (2)	238 (2)	1 (1)	567 (2)	237 (2)	0 (2)
H(9)	486 (2)	120 (2)	−108 (1)	483 (2)	118 (2)	−107 (2)
H(10)	377 (2)	18 (2)	−229 (1)	372 (2)	19 (2)	−224 (2)
H(11)	194 (2)	−62 (2)	−206 (1)	190 (2)	−60 (2)	−203 (2)
H(12)	141 (2)	−51 (2)	−60 (1)	136 (2)	−42 (2)	−57 (2)
H(15)	92 (2)	219 (2)	−16 (1)	97 (2)	221 (2)	−11 (2)
H(16)	−52 (2)	362 (2)	−11 (1)	−47 (2)	359 (2)	−8 (2)
H(17)	−142 (2)	380 (2)	118 (1)	−137 (2)	381 (2)	120 (1)
H(18)	−73 (2)	265 (2)	243 (2)	−71 (2)	262 (2)	243 (2)
H(21)	−6 (2)	134 (2)	348 (1)	−4 (2)	135 (2)	352 (1)
H(22)	97 (2)	30 (2)	469 (1)	96 (2)	28 (2)	470 (2)
H(23)	276 (2)	−56 (2)	446 (1)	272 (2)	−58 (2)	446 (2)
H(24)	335 (2)	−42 (2)	306 (1)	333 (2)	−48 (2)	305 (2)

	T = 165 K[a]			T = 296 K[a]		
	x	y	z	x	y	z
M(1)	2400.6 (4)	470.1 (4)	1240.1 (3)	2409.1 (5)	491.8 (5)	1259.3 (4)
N(2)	3939 (3)	1455 (3)	1397 (2)	3941 (3)	1482 (3)	1420 (2)
C(3)	4441 (4)	2019 (4)	2123 (3)	4440 (5)	2039 (5)	2155 (3)
C(4)	5397 (4)	2747 (4)	2119 (3)	5369 (5)	2756 (5)	2148 (4)
C(5)	5856 (4)	2879 (4)	1331 (3)	5823 (5)	2914 (5)	1370 (4)
C(6)	5349 (4)	2305 (4)	570 (3)	5320 (5)	2344 (5)	618 (4)
C(7)	4394 (3)	1592 (3)	625 (3)	4395 (4)	1630 (4)	665 (3)
C(8)	3766 (3)	952 (3)	−163 (2)	3756 (4)	993 (4)	−118 (3)
C(9)	4181 (4)	861 (3)	−988 (3)	4159 (4)	903 (4)	−933 (3)
C(10)	3491 (4)	284 (3)	−1683 (3)	3494 (5)	312 (4)	−1621 (3)
C(11)	2407 (4)	−172 (4)	−1549 (3)	2440 (5)	−143 (5)	−1496 (3)
C(12)	2065 (4)	−105 (4)	−709 (3)	2083 (5)	−63 (5)	−669 (3)
N(13)	2736 (3)	448 (3)	−22 (2)	2750 (3)	488 (3)	15 (2)
N(14)	1006 (3)	1658 (3)	1114 (2)	1013 (3)	1652 (3)	1145 (2)
C(15)	608 (4)	2325 (3)	415 (3)	594 (4)	2304 (4)	446 (3)
C(16)	−267 (4)	3127 (4)	439 (3)	−274 (5)	3087 (5)	473 (3)
C(17)	−784 (4)	3227 (4)	1209 (3)	−774 (5)	3185 (5)	1233 (4)
C(18)	−391 (4)	2537 (4)	1941 (3)	−377 (4)	2502 (4)	1945 (3)
C(19)	519 (3)	1769 (3)	1874 (3)	522 (4)	1754 (4)	1897 (3)
C(20)	1070 (3)	1054 (3)	2645 (3)	1086 (4)	1046 (4)	2650 (3)
C(21)	626 (4)	968 (4)	3450 (3)	658 (4)	947 (5)	3447 (3)
C(22)	1255 (4)	329 (4)	4140 (3)	1282 (5)	315 (5)	4120 (3)
C(23)	2300 (4)	−203 (4)	4015 (3)	2309 (5)	−202 (5)	3997 (3)
C(24)	2673 (4)	−122 (4)	3185 (3)	2695 (5)	−115 (5)	3183 (3)

Table II (Continued)

	T = 165 K[a]			T = 296 K[a]		
	x	y	z	x	y	z
N(25)	2064 (3)	491 (3)	2505 (2)	2076 (3)	498 (3)	2511 (2)
O(26)	1300 (3)	−1067 (3)	1060 (2)	1318 (4)	−1064 (4)	1069 (3)
O(27)	3112 (3)	−1381 (4)	1431 (2)	3115 (3)	−1320 (4)	1430 (3)
N(28)	2090 (4)	−1798 (3)	1253 (2)	2117 (4)	−1760 (4)	1248 (3)
O(29)	−2106 (3)	290 (3)	3726 (2)	−2134 (3)	293 (3)	3689 (3)
O(30)	−3842 (3)	1015 (3)	3829 (2)	−3811 (3)	976 (4)	3838 (3)
O(31)	−2311 (3)	2077 (3)	3748 (3)	−2319 (4)	2011 (4)	3806 (4)
N(32)	−2763 (3)	1131 (3)	3768 (2)	−2749 (4)	1102 (4)	3780 (3)
H(3)	412 (3)	186 (3)	263 (2)	406 (3)	195 (3)	263 (2)
H(4)	569 (4)	307 (4)	268 (3)	561 (4)	308 (4)	265 (3)
H(5)	646 (6)	335 (6)	129 (4)	639 (4)	340 (4)	139 (3)
H(6)	562 (4)	237 (3)	5 (3)	567 (4)	248 (4)	16 (3)
H(9)	490 (3)	113 (3)	−106 (2)	474 (3)	113 (3)	−101 (2)
H(10)	377 (4)	19 (4)	−220 (3)	376 (4)	26 (4)	−220 (3)
H(11)	191 (4)	−58 (4)	−201 (3)	193 (4)	−53 (4)	−190 (3)
H(12)	132 (3)	−46 (3)	−60 (2)	140 (4)	−32 (4)	−54 (3)
H(15)	92 (4)	224 (3)	−14 (3)	98 (3)	219 (3)	1 (2)
H(16)	−43 (4)	354 (4)	−13 (3)	−42 (4)	358 (4)	2 (3)
H(17)	−133 (4)	378 (4)	132 (3)	−133 (3)	363 (3)	134 (2)
H(18)	−67 (3)	260 (3)	247 (3)	−69 (3)	258 (3)	243 (2)
H(21)	−12 (4)	137 (4)	350 (3)	0 (3)	129 (3)	351 (2)
H(22)	93 (4)	27 (4)	468 (3)	99 (4)	27 (4)	468 (3)
H(23)	270 (4)	−58 (3)	441 (3)	264 (4)	−55 (4)	433 (3)
H(24)	334 (4)	−50 (3)	309 (3)	335 (4)	−51 (4)	310 (3)

	T = 295 K[b]				T = 295 K[b]		
	x	y	z		x	y	z
M(1)	2397.4 (4)	506.6 (4)	1255.0 (3)	N(25)	2113 (3)	563 (3)	2586 (2)
N(2)	3936 (3)	1497 (3)	1374 (2)	O(26)	1279 (3)	−1035 (3)	1053 (2)
C(3)	4442 (4)	2062 (4)	2104 (3)	O(27)	3138 (3)	−1198 (3)	1471 (2)
C(4)	5370 (5)	2780 (5)	2109 (4)	N(28)	2149 (4)	−1685 (3)	1269 (3)
C(5)	5804 (4)	2926 (4)	1349 (4)	O(29)	−2159 (3)	318 (3)	3728 (2)
C(6)	5295 (4)	2364 (4)	601 (4)	O(30)	−3816 (4)	1054 (4)	3841 (2)
C(7)	4365 (3)	1647 (3)	623 (3)	O(31)	−2331 (4)	2038 (4)	3668 (4)
C(8)	3734 (3)	1003 (3)	−157 (2)	N(32)	−2758 (4)	1149 (4)	3760 (2)
C(9)	4176 (4)	886 (4)	−940 (3)	H(3)	411 (3)	184 (4)	260 (3)
C(10)	3519 (4)	307 (4)	−1632 (3)	H(4)	560 (3)	311 (3)	260 (3)
C(11)	2448 (5)	−149 (4)	−1552 (3)	H(5)	630 (3)	329 (3)	138 (3)
C(12)	2066 (5)	−31 (5)	−761 (3)	H(6)	559 (4)	241 (4)	12 (3)
N(13)	2705 (3)	523 (3)	−65 (2)	H(9)	487 (3)	115 (3)	−97 (2)
N(14)	1004 (3)	1669 (3)	1164 (2)	H(10)	385 (3)	206 (3)	−219 (3)
C(15)	578 (4)	2316 (4)	459 (3)	H(11)	198 (4)	−52 (4)	−202 (3)
C(16)	−286 (4)	3099 (4)	442 (4)	H(12)	155 (3)	−38 (3)	−70 (3)
C(17)	−758 (4)	3208 (4)	1194 (3)	H(15)	90 (3)	224 (3)	4 (3)
C(18)	−356 (4)	2559 (4)	1937 (4)	H(16)	−45 (4)	367 (4)	1 (3)
C(19)	533 (3)	1799 (3)	1896 (3)	H(17)	−112 (3)	362 (3)	124 (2)
C(20)	1104 (3)	1093 (3)	2672 (2)	H(18)	−67 (4)	278 (4)	246 (3)
C(21)	624 (4)	997 (4)	3428 (3)	H(21)	−9 (4)	136 (3)	343 (3)
C(22)	1250 (5)	366 (4)	4112 (3)	H(22)	102 (3)	28 (3)	458 (3)
C(23)	2302 (5)	−157 (5)	4045 (3)	H(23)	289 (5)	−56 (4)	451 (4)
C(24)	2703 (4)	−44 (5)	3268 (3)	H(24)	344 (4)	−37 (4)	322 (3)

[a] M(1) = Cu(1). [b] M(1) = Zn(1). [c] esd's are in parentheses.

assume that the causes of the structural and vibrational differences are not due to crystal-packing forces.

Structural Results of Other $[ML_2(OXO)]Y$ Complexes. Besides $[Cu(bpy)_2(ONO)]NO_3$ and $[Zn(bpy)_2(ONO)]NO_3$, other $[ML_2(OXO)]Y$ structures have been reported; the metal–ligand bond lengths are given in Table IV. Three major observations can be made:[10,32] [1] The geometry of the CuN_4O_2 chromophore varies significantly, even when the cation is unchanged. For example, the Cu–O bond lengths in $[Cu(phen)_2(CH_3CO_2)]ClO_4$ are 2.220 (4) and 2.421 (5) Å (T = 298 K),[10] while the corresponding bonds in $[Cu(phen)_2(CH_3CO_2)]BF_4$ are 1.996 (2) and 2.670 (3) Å (T = 298 K).[33] [2] The pattern of distortion from C_2 symmetry in the Cu compounds is systematic: (a) as one Cu–O bond lengthens, the other shortens; (b) as a Cu–O bond lengthens (or shortens), the Cu–N bond trans to it also lengthens (or shortens) in parallel but by a considerably smaller amount; (c) again in parallel, the Cu–N (axial) bond *within the same ligand* lengthens or shortens together with the Cu–N (equatorial) bond by an even smaller amount. [Note that this form of distortion is observed for $[Cu(bpy)_2(ONO)]NO_3$ (but not for the Zn(II) analogue): the trans equatorial Cu(1)–O(27) and Cu(1)–N(14) bonds are longer than the other trans equatorial Cu(1)–O(26) and Cu(1)–N(2) bonds, and the axial Cu(1)–N(13) and Cu(1)–N(25) bonds are slightly unequal.] [3] The structure of the CuN_4O_2 chromophore is temperature dependent. The Cu(1)–O(26) and Cu(1)–O(27) bond lengths in $[Cu(bpy)_2(ONO)]NO_3$ are 2.051 (2) and 2.536 (2) Å at T = 20 K and 2.230 (5) and 2.320 (5) Å at 296 K (see Table III).

ORTEP drawings of the equatorial atoms of all complexes cited in Table IV are shown in Figure 2, and a summary of the anisotropic Gaussian displacement parameters for these atoms is given in Table V. Of particular interest are the Gaussian ellipsoids for the O atoms of the coordinated anions and the way these ellipsoids vary as the Cu–O coordination geometry changes. For example, in the group of $[CuL_2(CH_3CO_2)]Y$ complexes, the O

(32) Simmons, C. J.; Seff, K.; Clifford, F.; Hathaway, B. *Acta Crystallogr. Sect. C: Cryst. Struct. Commun.* **1983**, *C39*, 1360.
(33) Fitzgerald, W.; Hathaway, B. *Acta Crystallogr., Sect. C: Cryst. Struct. Commun.* **1984**, *C40*, 243.

Table III. Bond Lengths (Å) and Angles (deg) Involving Non-hydrogen Atoms[c]

	T = 20 K[a]	T = 100 K[a]	T = 165 K[a]	T = 296 K[a]	T = 295 K[b]
			A. Bond Lengths		
M(1)-N(2)	2.028 (2)	2.060 (2)	2.071 (2)	2.074 (4)	2.082 (3)
M(1)-N(13)	1.982 (2)	1.986 (2)	1.984 (2)	1.980 (3)	2.126 (3)
M(1)-N(14)	2.142 (2)	2.110 (2)	2.098 (2)	2.085 (4)	2.085 (3)
M(1)-N(25)	1.998 (2)	1.992 (2)	1.989 (2)	1.988 (3)	2.135 (3)
M(1)-O(26)	2.051 (2)	2.155 (2)	2.204 (3)	2.230 (5)	2.223 (3)
M(1)-O(27)	2.536 (2)	2.414 (2)	2.351 (3)	2.320 (5)	2.204 (3)
N(2)-C(3)	1.342 (3)	1.339 (3)	1.326 (4)	1.337 (6)	1.340 (6)
N(2)-C(7)	1.359 (3)	1.355 (3)	1.345 (3)	1.336 (5)	1.349 (5)
C(3)-C(4)	1.381 (3)	1.374 (4)	1.381 (4)	1.355 (8)	1.354 (7)
C(4)-C(5)	1.386 (3)	1.381 (4)	1.369 (5)	1.369 (9)	1.363 (8)
C(5)-C(6)	1.385 (3)	1.382 (4)	1.373 (5)	1.367 (8)	1.360 (8)
C(6)-C(7)	1.383 (3)	1.384 (4)	1.381 (4)	1.358 (7)	1.362 (6)
C(7)-C(8)	1.482 (3)	1.478 (4)	1.486 (4)	1.491 (6)	1.487 (6)
C(8)-C(9)	1.389 (3)	1.388 (4)	1.391 (4)	1.384 (6)	1.398 (6)
C(8)-N(13)	1.347 (3)	1.343 (3)	1.349 (3)	1.327 (5)	1.327 (5)
C(9)-C(10)	1.380 (3)	1.375 (4)	1.379 (4)	1.374 (7)	1.362 (6)
C(10)-C(11)	1.379 (3)	1.379 (4)	1.375 (4)	1.345 (7)	1.353 (7)
C(11)-C(12)	1.389 (3)	1.385 (4)	1.375 (4)	1.377 (7)	1.375 (7)
C(12)-N(13)	1.338 (3)	1.342 (3)	1.346 (3)	1.346 (6)	1.344 (6)
N(14)-C(15)	1.340 (3)	1.334 (3)	1.333 (4)	1.336 (6)	1.343 (6)
N(14)-C(19)	1.353 (3)	1.355 (3)	1.345 (3)	1.348 (5)	1.343 (5)
C(15)-C(16)	1.385 (3)	1.383 (4)	1.377 (4)	1.362 (7)	1.350 (7)
C(16)-C(17)	1.382 (3)	1.382 (4)	1.376 (4)	1.365 (8)	1.372 (7)
C(17)-C(18)	1.387 (3)	1.382 (4)	1.386 (4)	1.368 (8)	1.383 (7)
C(18)-C(19)	1.390 (3)	1.389 (4)	1.387 (4)	1.363 (6)	1.365 (6)
C(19)-C(20)	1.489 (3)	1.484 (4)	1.488 (4)	1.477 (6)	1.502 (5)
C(20)-C(21)	1.388 (3)	1.379 (4)	1.378 (4)	1.374 (6)	1.378 (6)
C(20)-N(25)	1.352 (3)	1.356 (3)	1.347 (3)	1.339 (5)	1.333 (5)
C(21)-C(22)	1.382 (3)	1.380 (4)	1.384 (4)	1.367 (7)	1.374 (7)
C(22)-C(23)	1.381 (3)	1.373 (4)	1.372 (5)	1.349 (8)	1.364 (8)
C(23)-C(24)	1.378 (3)	1.379 (4)	1.376 (4)	1.375 (8)	1.365 (7)
C(24)-N(25)	1.342 (3)	1.339 (3)	1.347 (4)	1.350 (6)	1.342 (6)
O(26)-N(28)	1.283 (2)	1.261 (3)	1.245 (4)	1.225 (6)	1.246 (5)
O(27)-N(28)	1.248 (2)	1.238 (3)	1.240 (4)	1.228 (6)	1.245 (5)
O(29)-N(32)	1.263 (2)	1.261 (3)	1.253 (3)	1.215 (5)	1.209 (6)
O(30)-N(32)	1.261 (2)	1.252 (3)	1.237 (3)	1.219 (5)	1.229 (6)
O(31)-N(32)	1.254 (2)	1.249 (3)	1.240 (3)	1.195 (6)	1.189 (6)
			B. Bond Angles		
N(2)-M(1)-N(13)	81.22 (7)	80.70 (8)	80.50 (9)	80.0 (2)	77.9 (1)
N(2)-M(1)-N(14)	100.68 (7)	102.08 (8)	102.85 (9)	102.8 (1)	103.4 (1)
N(2)-M(1)-N(25)	98.25 (7)	99.07 (8)	99.53 (9)	99.8 (2)	100.1 (1)
N(2)-M(1)-O(26)	160.72 (7)	158.90 (8)	158.01 (9)	157.7 (2)	157.9 (1)
N(2)-M(1)-O(27)	107.56 (6)	105.81 (8)	105.03 (8)	105.4 (1)	103.1 (1)
N(13)-M(1)-N(14)	101.48 (7)	100.30 (8)	100.05 (9)	100.6 (1)	101.0 (1)
N(13)-M(1)-N(25)	178.91 (7)	179.63 (8)	179.96 (9)	179.7 (2)	177.5 (1)
N(13)-M(1)-O(26)	92.75 (7)	93.48 (8)	93.42 (9)	93.7 (2)	93.9 (1)
N(13)-M(1)-O(27)	89.76 (6)	89.82 (8)	89.51 (8)	89.3 (1)	91.4 (1)
N(14)-M(1)-N(25)	79.55 (7)	80.03 (8)	79.97 (9)	79.6 (2)	77.9 (1)
N(14)-M(1)-O(26)	98.47 (6)	98.91 (8)	99.01 (9)	99.3 (2)	98.2 (1)
N(14)-M(1)-O(27)	150.91 (6)	151.53 (7)	151.66 (9)	151.3 (2)	152.4 (1)
N(25)-M(1)-O(26)	87.45 (7)	86.63 (8)	86.53 (9)	86.5 (2)	88.5 (1)
N(25)-M(1)-O(27)	89.49 (6)	89.96 (8)	90.44 (8)	90.7 (2)	90.5 (1)
O(26)-M(1)-O(27)	53.83 (5)	53.62 (7)	53.51 (9)	52.8 (2)	56.1 (1)
M(1)-N(2)-C(3)	127.1 (2)	127.7 (2)	128.3 (2)	127.6 (4)	125.0 (3)
M(1)-N(2)-C(7)	114.0 (1)	113.2 (2)	113.2 (2)	113.7 (3)	115.6 (2)
C(3)-N(2)-C(7)	118.7 (2)	118.9 (2)	118.3 (3)	118.4 (4)	119.1 (3)
N(2)-C(3)-C(4)	122.6 (2)	122.8 (2)	123.0 (3)	121.9 (6)	121.9 (5)
C(3)-C(4)-C(5)	118.5 (2)	118.4 (3)	118.3 (3)	119.5 (6)	118.9 (5)
C(4)-C(5)-C(6)	119.5 (2)	119.6 (3)	119.7 (3)	118.8 (6)	119.9 (5)
C(5)-C(6)-C(7)	119.1 (2)	119.2 (3)	118.7 (3)	119.2 (6)	119.5 (5)
N(2)-C(7)-C(6)	121.5 (2)	121.1 (2)	122.0 (3)	122.1 (5)	120.7 (4)
N(2)-C(7)-C(8)	114.0 (2)	114.6 (2)	115.1 (2)	114.1 (4)	115.3 (3)
C(6)-C(7)-C(8)	124.5 (2)	124.2 (2)	122.9 (3)	123.7 (5)	123.9 (4)
C(7)-C(8)-C(9)	123.5 (2)	123.7 (2)	124.2 (3)	124.2 (4)	123.5 (3)
C(7)-C(8)-N(13)	115.1 (2)	115.2 (2)	114.4 (2)	115.1 (4)	115.5 (3)
C(9)-C(8)-N(13)	121.4 (2)	121.1 (2)	121.4 (2)	120.7 (4)	121.0 (4)
C(8)-C(9)-C(10)	118.8 (2)	119.1 (2)	118.8 (3)	119.8 (5)	119.4 (4)
C(9)-C(10)-C(11)	119.8 (2)	119.8 (2)	119.5 (3)	119.0 (5)	119.7 (4)
C(10)-C(11)-C(12)	118.5 (2)	118.4 (3)	119.4 (3)	119.5 (5)	118.5 (5)
C(11)-C(12)-N(13)	121.9 (2)	121.9 (2)	121.6 (3)	121.5 (5)	122.9 (5)
M(1)-N(13)-C(8)	115.3 (2)	115.7 (2)	116.1 (2)	116.5 (3)	114.5 (2)

Table III (Continued)

	T = 20 K[a]	T = 100 K[a]	T = 165 K[a]	T = 296 K[a]	T = 295 K[b]
M(1)-N(13)-C(12)	125.0 (2)	124.7 (2)	124.5 (2)	124.1 (3)	126.4 (3)
C(8)-N(13)-C(12)	119.4 (2)	119.5 (2)	119.2 (2)	119.2 (4)	118.3 (4)
M(1)-N(14)-C(15)	128.6 (2)	128.5 (2)	128.7 (2)	128.3 (3)	125.8 (3)
M(1)-N(14)-C(19)	112.3 (2)	112.5 (2)	112.8 (2)	113.4 (3)	115.9 (2)
C(15)-N(14)-C(19)	119.0 (2)	118.9 (2)	118.4 (2)	118.3 (4)	118.2 (3)
N(14)-C(15)-C(16)	122.4 (2)	122.7 (2)	123.1 (3)	122.9 (5)	124.0 (4)
C(15)-C(16)-C(17)	118.8 (2)	118.6 (3)	118.7 (3)	118.7 (6)	116.5 (5)
C(16)-C(17)-C(18)	119.2 (2)	119.3 (3)	119.2 (3)	119.0 (6)	121.7 (4)
C(17)-C(18)-C(19)	119.1 (2)	119.2 (2)	118.8 (3)	120.1 (6)	117.6 (5)
N(14)-C(19)-C(18)	121.4 (2)	121.2 (2)	121.9 (3)	121.0 (5)	121.9 (4)
N(14)-C(19)-C(20)	114.9 (2)	115.0 (2)	115.2 (2)	114.5 (4)	115.0 (3)
C(18)-C(19)-C(20)	123.7 (2)	123.6 (2)	122.8 (3)	124.5 (4)	123.0 (4)
C(19)-C(20)-C(21)	123.3 (2)	123.9 (2)	123.9 (3)	123.9 (4)	122.6 (4)
C(19)-C(20)-N(25)	115.7 (2)	115.2 (2)	114.7 (2)	115.1 (4)	115.6 (3)
C(21)-C(20)-N(25)	121.0 (2)	121.0 (2)	121.4 (3)	121.0 (4)	121.8 (4)
C(20)-C(21)-C(22)	119.2 (2)	119.1 (2)	118.8 (3)	119.3 (5)	117.6 (4)
C(21)-C(22)-C(23)	119.6 (2)	119.9 (3)	120.0 (3)	119.9 (5)	121.4 (5)
C(22)-C(23)-C(24)	118.6 (2)	118.4 (3)	118.6 (3)	119.4 (6)	117.5 (5)
C(23)-C(24)-C(25)	122.3 (2)	122.4 (3)	122.0 (3)	121.0 (6)	122.7 (5)
M(1)-N(25)-C(20)	116.0 (2)	115.8 (2)	116.2 (2)	116.3 (2)	113.6 (2)
M(1)-N(25)-C(24)	123.6 (2)	124.4 (2)	124.2 (2)	124.0 (3)	126.0 (3)
C(20)-N(25)-C(24)	119.2 (2)	119.1 (2)	119.1 (2)	119.2 (4)	119.0 (3)
M(1)-O(26)-N(28)	107.4 (2)	103.1 (2)	101.0 (2)	100.3 (3)	94.8 (3)
M(1)-O(27)-N(28)	84.9 (2)	91.0 (2)	93.8 (2)	95.7 (3)	95.7 (3)
O(26)-N(28)-O(27)	113.9 (2)	112.2 (2)	111.6 (3)	111.2 (5)	113.4 (4)
O(29)-N(32)-O(30)	119.5 (2)	119.8 (2)	120.3 (3)	119.3 (5)	119.4 (4)
O(29)-N(32)-O(31)	119.9 (2)	119.5 (2)	118.9 (3)	120.3 (5)	119.2 (4)
O(30)-N(32)-O(31)	120.6 (2)	120.7 (2)	120.8 (3)	120.4 (5)	121.3 (5)

[a] M(1) = Cu(1). [b] M(1) = Zn(1). [c] esd's are in parentheses.

Table IV. Molecular Geometries of [M(bpy or phen)$_2$(OXO)]Y Complexes (M = Cu, Zn)[a]

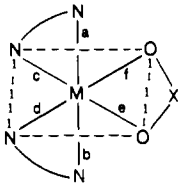

	complex	space group	a (Å)	b (Å)	c (Å)	d (Å)	e (Å)	f (Å)	S[c] (Å)	ref
(1)[b]	$[Cu(bpy)_2(CH_3CO_2)]BF_4$	$P2_1/c$	1.995 (6)	2.016 (6)	2.033 (5)	2.209 (6)	1.980 (4)	2.785 (5)	1.00 (1)	*d*
(2)	$[Cu(phen)_2(CH_3CO_2)]BF_4$	$P\bar{1}$	2.010 (2)	2.025 (2)	2.062 (2)	2.218 (2)	1.996 (2)	2.670 (3)	0.84 (1)	*e*
(3)	$[Cu(bpy)_2(CH_3CO_2)]ClO_4 \cdot H_2O$	$P\bar{1}$	1.971 (5)	1.994 (5)	2.056 (5)	2.168 (5)	2.031 (5)	2.648 (5)	0.75 (1)	*d*
(4)	$[Cu(phen)_2(CH_3CO_2)]NO_3 \cdot 2H_2O$	$P\bar{1}$	2.000 (3)	2.019 (3)	2.083 (3)	2.170 (3)	2.123 (5)	2.448 (5)	0.43 (1)	*f*
(5)	$[Cu(phen)_2(CH_3CO_2)]ClO_4$	$P2_1/c$	2.002 (2)	2.012 (3)	2.097 (3)	2.141 (3)	2.155 (4)	2.528 (4)	0.44 (1)[g]	*h*
(6)	$[Cu(phen)_2(CH_3CO_2)]ClO_4$	$P2_1/c$	1.994 (4)	2.006 (4)	2.098 (4)	2.130 (4)	2.220 (4)	2.421 (5)	0.25 (1)	*h*
(7)	$[Cu(phen)_2(CH_3CO_2)]ClO_4 \cdot 2H_2O$	$P2/c$	1.999 (2)	1.999 (2)	2.122 (2)	2.122 (2)	2.252 (3)	2.252 (3)	0.00 (0)	*f*
(8)	$[Cu(phen)_2(CH_3CO_2)]BF_4 \cdot 2H_2O$	$P2/c$	2.000 (4)	2.000 (4)	2.123 (4)	2.123 (4)	2.261 (5)	2.261 (5)	0.00 (0)	*i*
	$[Zn(phen)_2(CH_3CO_2)]BF_4 \cdot 2H_2O$	$P2/c$	2.147 (2)	2.147 (2)	2.116 (2)	2.116 (2)	2.184 (2)	2.184 (2)	0.00 (0)	*f*
(9)	$[Cu(phen)_2(ONO)]BF_4$	$P\bar{1}$	1.999 (4)	2.019 (3)	2.049 (3)	2.167 (3)	2.072 (4)	2.597 (4)	0.66 (1)	*i*
(10)	$[Cu(bpy)_2(ONO)]BF_4$	$P2_1/c$	1.990 (5)	2.004 (5)	2.052 (5)	2.142 (5)	2.117 (6)	2.462 (6)	0.45 (1)	*j*
(11)	$[Cu(bpy)_2(ONO)]PF_6$	$P\bar{1}$	1.991 (3)	1.993 (3)	2.092 (3)	2.134 (3)	2.178 (5)	2.429 (5)	0.29 (1)	*k*
(12)	$[Cu(bpy)_2(ONO)]NO_3$	$P2_1/c$	1.983 (2)	1.998 (2)	2.028 (2)	2.142 (2)	2.051 (2)	2.536 (2)	0.61 (1)[l]	*m*
(13)	$[Cu(bpy)_2(ONO)]NO_3$	$P2_1/c$	1.986 (2)	1.992 (2)	2.060 (2)	2.110 (2)	2.155 (2)	2.414 (2)	0.32 (1)[n]	*m*
(14)	$[Cu(bpy)_2(ONO)]NO_3$	$P2_1/c$	1.984 (2)	1.989 (2)	2.071 (2)	2.098 (2)	2.204 (3)	2.351 (3)	0.18 (1)[o]	*p*
(15)	$[Cu(bpy)_2(ONO)]NO_3$	$P2_1/c$	1.980 (3)	1.988 (3)	2.074 (4)	2.085 (4)	2.230 (5)	2.320 (5)	0.11 (1)	*p,q*
	$[Zn(bpy)_2(ONO)]NO_3$	$P2_1/c$	2.126 (3)	2.135 (3)	2.082 (3)	2.085 (3)	2.223 (3)	2.204 (3)	0.03 (1)	*j,m*
(16)	$[Cu(bpy)_2(HCO_2)]BF_4 \cdot {}^1/_2H_2O$	$P\bar{1}$	1.978 (5)	2.001 (5)	2.061 (5)	2.158 (5)	2.024 (5)	2.869 (12)	0.97 (2)	*r*
(17)	$[Cu(phen)_2(HCO_2)]BF_4$	$C2/c$	1.990 (6)	1.990 (6)	2.111 (6)	2.111 (6)	2.363 (8)	2.363 (8)	0.00 (0)	*s*
(18)	$[Cu(phen)_2(HCO_2)]ClO_4$	$C2/c$	1.985 (3)	1.985 (3)	2.111 (3)	2.111 (3)	2.353 (6)	2.353 (6)	0.00 (0)	*t*

[a] All structures determined at room temperature unless indicated otherwise. [b] The numbers used in this table serve to identify the points in Figure 4. [c] S = (b − a) + (d − c) + (f − e) or equivalently $S = \Delta d(Cu\text{-}N_{ax}) + \Delta d(Cu\text{-}N_{eq}) + \Delta d(Cu\text{-}O_{eq})$; it is a measure of the amount of distortion from C_2 symmetry. [d] Hathaway, B. J.; Ray, N.; Kennedy, D.; O'Brien, N.; Murphy, B. *Acta Crystallogr., Sect. B: Struct. Crystallogr. Cryst. Chem.* **1980**, *B36*, 1371. [e] Fitzgerald, W.; Hathaway, B. *Acta Crystallogr., Sect. C: Cryst. Struct. Commun.* **1984**, *C40*, 243. [f] Fitzgerald, W.; Hathaway, B.; Simmons, C. J. *J. Chem. Soc., Dalton Trans.* **1985**, 141. [g] T = 173 K. [h] Simmons, C. J.; Alcock, N. W.; Seff, K.; Fitzgerald, W.; Hathaway, B. J. *Acta Crystallogr., Sect. B: Struct. Crystallogr. Cryst. Chem.* **1985**, *B41*, 42. [i] Simmons, C. J.; Seff, K.; Clifford, F.; Hathaway, B. J. *Acta Crystallogr., Sect. C: Cryst. Struct. Commun.* **1983**, *C39*, 1360. [j] Walsh, A.; Walsh, B.; Murphy, B.; Hathaway, B. J. *Acta Crystallogr., Sect. B: Struct. Crystallogr. Cryst. Chem.* **1981**, *B37*, 1512. [k] Tyagi, S.; Hathaway, B. J., unpublished results. [l] T = 20 K. [m] This work. [n] T = 100 K. [o] T = 165 K. [p] Simmons, C. J.; Clearfield, A.; Fitzgerald, W.; Tyagi, S.; Hathaway, B. J. *Inorg. Chem.* **1983**, *22*, 2463. Simmons, C.; Clearfield, A.; Fitzgerald, W.; Tyagi, S.; Hathaway, B. *J. Chem. Soc., Chem. Commun.* **1983**, 189. Simmons, C. J.; Clearfield, A.; Fitzgerald, W.; Tyagi, S.; Hathaway, B. J. *Trans. Am. Cryst. Assoc.* **1984**, *20*, 155. [q] Procter, I. M.; Stephens, F. S. *J. Chem. Soc. A* **1969**, 1248. [r] Fitzgerald, W.; Hathaway, B. J. *J. Chem. Soc., Dalton Trans.* **1981**, 567. [s] Hathaway, B. J.; unpublished results. [t] Escobar, C.; Wittke, O. *Acta Crystallogr., Sect. C.: Cryst. Struct. Commun.* **1983**, *C39*, 1643.

Table V. Room Temperature Root-Mean-Square Values, $U_i^{1/2}$ (Å), of Principal Axes of Gaussian Ellipsoids of Equatorial Atoms in $[ML_2(OXO)]Y$ Complexes in Table IV[d]

complex	atom[a]	$U_1^{1/2}$ (Å)	$U_2^{1/2}$	$U_3^{1/2}$	γ_3, deg	$\Delta U^{1/2}(M - L_i)$[b,c]
$[Cu(bpy)_2(CH_3CO_2)]BF_4$	O_l	0.20	0.25	0.28	27.5	0.16
	O_s	0.19	0.22	0.23	63.0	0.03
	N_l	0.19	0.22	0.25	68.6	0.02
	N_s	0.18	0.20	0.21	66.5	0.03
	M	0.16	0.21	0.22		
$[Cu(phen)_2(CH_3CO_2)]BF_4$	O_l	0.21	0.29	0.36	54.5	0.23
	O_s	0.21	0.23	0.24	43.2	0.12
	N_l	0.18	0.20	0.21	47.5	−0.05
	N_s	0.19	0.20	0.22	51.2	0.07
	M	0.17	0.20	0.22		
$[Cu(bpy)_2(CH_3CO_2)]ClO_4 \cdot H_2O$	O_l	0.18	0.29	0.38	58.3	0.24
	O_s	0.20	0.22	0.27	76.6	0.09
	N_l	0.18	0.21	0.23	36.5	0.05
	N_s	0.20	0.20	0.21	68.4	0.05
	M	0.18	0.20	0.22		
$[Cu(phen)_2(CH_3CO_2)]NO_3 \cdot 2H_2O$	O_l	0.22	0.26	0.39	11.3	0.33
	O_s	0.21	0.23	0.37	15.6	0.30
	N_l	0.19	0.21	0.22	74.5	0.06
	N_s	0.18	0.19	0.22	17.9	0.08
	M	0.18	0.19	0.20		
$[Cu(phen)_2(CH_3CO_2)]ClO_4$	O_l	0.20	0.29	0.56	18.1	0.49
	O_s	0.24	0.27	0.42	25.4	0.33
	N_l	0.19	0.20	0.23	73.5	−0.08
	N_s	0.20	0.21	0.23	85.5	0.04
	M	0.18	0.21	0.23		
$[Cu(phen)_2(CH_3CO_2)]ClO_4 \cdot 2H_2O$	O	0.24	0.26	0.41	7.1	0.34
	O	0.24	0.26	0.41	7.1	0.34
	N	0.21	0.22	0.25	63.3	0.05
	N	0.21	0.22	0.25	63.3	0.05
	M	0.20	0.22	0.23		
$[Cu(phen)_2(CH_3CO_2)]BF_4 \cdot 2H_2O$	O	0.23	0.26	0.42	13.4	0.34
	O	0.23	0.26	0.42	13.4	0.34
	N	0.21	0.22	0.24	65.5	0.01
	N	0.21	0.22	0.24	65.5	0.01
	M	0.20	0.21	0.25		
$[Zn(phen)_2(CH_3CO_2)]BF_4 \cdot 2H_2O$	O	0.24	0.26	0.28	85.3	0.15
	O	0.24	0.26	0.28	85.3	0.15
	N	0.22	0.23	0.24	26.6	0.10
	N	0.22	0.23	0.24	26.6	0.10
	M	0.18	0.21	0.21		
$[Cu(phen)_2(ONO)]BF_4$	O_l	0.24	0.26	0.39	32.0	0.27
	O_s	0.24	0.25	0.30	63.5	0.14
	N_l	0.20	0.21	0.23	37.2	−0.05
	N_s	0.20	0.23	0.24	86.0	0.07
	M	0.18	0.21	0.24		
$[Cu(bpy)_2(ONO)]BF_4$	O_l	0.25	0.30	0.35	26.4	0.25
	O_s	0.26	0.28	0.33	48.3	0.21
	N_l	0.20	0.22	0.24	44.8	0.06
	N_s	0.18	0.22	0.23	43.4	0.04
	M	0.18	0.22	0.23		
$[Cu(bpy)_2(ONO)]PF_6$	O_l	0.23	0.30	0.36	20.4	0.27
	O_s	0.22	0.26	0.36	19.5	0.26
	N_l	0.17	0.21	0.24	63.3	0.04
	N_s	0.17	0.19	0.22	78.5	−0.04
	M	0.16	0.19	0.24		
$[Cu(bpy)_2(ONO)]NO_3$	O_l	0.25	0.28	0.35	16.2	0.27
	O_s	0.25	0.29	0.35	24.1	0.26
	N_l	0.18	0.21	0.22	38.9	−0.02
	N_s	0.20	0.21	0.22	65.9	−0.06
	M	0.18	0.21	0.22		
$[Zn(bpy)_2(ONO)]NO_3$	O_l	0.23	0.26	0.29	75.6	0.08
	O_s	0.24	0.25	0.28	77.9	0.11
	N_l	0.19	0.20	0.20	89.9	−0.06
	N_s	0.19	0.21	0.22	61.7	−0.06
	M	0.17	0.21	0.22		
$[Cu(bpy)_2(HCO_2)]BF_4 \cdot {}^1/_2H_2O$	O_l	0.23	0.30	0.40	47.0	0.25
	O_s	0.20	0.25	0.28	76.0	0.07
	N_l	0.20	0.22	0.24	76.9	−0.04
	N_s	0.20	0.21	0.24	66.2	0.04
	M	0.19	0.21	0.24		
$[Cu(phen)_2(HCO_2)]BF_4$	O	0.21	0.29	0.49	2.9	0.43
	O	0.21	0.29	0.49	2.9	0.43
	N	0.19	0.21	0.23	55.9	0.04
	N	0.19	0.21	0.23	55.9	0.04
	M	0.19	0.20	0.24		

Table V (Continued)

complex	atom[a]	$U_1^{1/2}$ (Å)	$U_2^{1/2}$	$U_3^{1/2}$	γ_3, deg	$\Delta U^{1/2}(M-L_i)^{b,c}$
$[Cu(phen)_2(HCO_2)]ClO_4$	O	0.22	0.27	0.49	4.7	0.43
	O	0.22	0.27	0.49	4.7	0.43
	N	0.18	0.20	0.22	37.8	0.04
	N	0.18	0.20	0.22	37.8	0.04
	M	0.18	0.20	0.24		

[a] O_l and N_l and O_s and N_s refer to those L_i ligand atoms involved in longer and shorter M–L_i bonds, respectively; see Table IV. [b] $\Delta U^{1/2}(M-L_i) = [U(L_i) - U(M)]^{1/2}$ in Å. [c] A negative sign indicates that $U(L_i) < U(M)$. [d] Angles, γ_3, between major axes of Gaussian ellipsoids and M–L_i bond vectors, and root-mean-square vibrational amplitudes, $\Delta U^{1/2}(M-L_i)$, along M–L_i bonds.

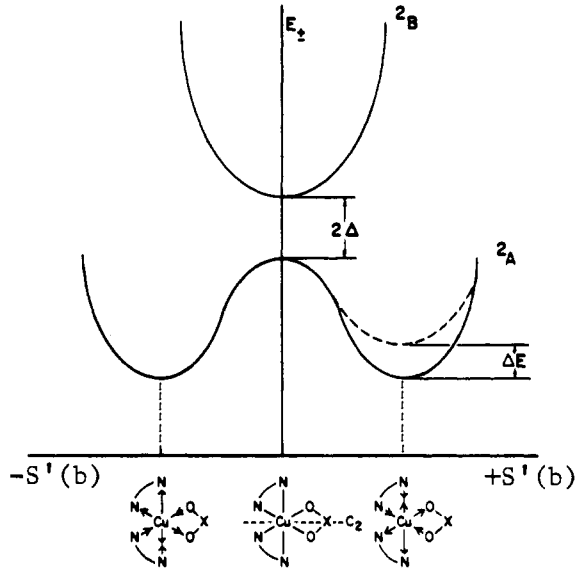

Figure 3. Proposed adiabatic potential energy surface model for the pseudodegenerate ^2A ground and ^2B excited electronic states in $[CuL_2(OXO)]Y$ systems based on theory and the crystallographic results reported herein. Vibronic levels not shown.

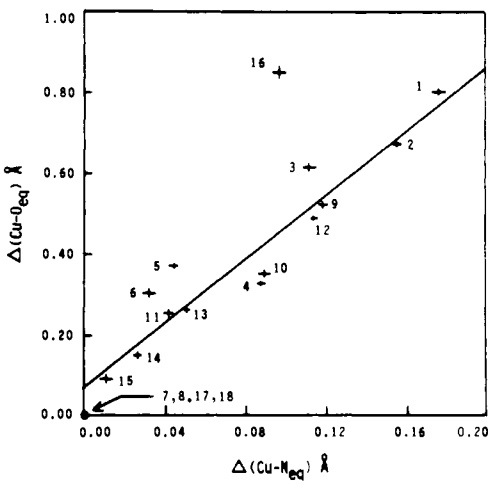

Figure 4. Plot of $\Delta d(Cu-O)_{eq}$ vs. $\Delta d(Cu-N)_{eq}$ (data numbering scheme of Table IV). The reasonably good least-squares line obtained is consistent with one distortional mode, the form of which is shown below the energy minima in Figure 3. Because complexes 7, 8, 17, and 18 have average C_2 symmetries, they were excluded from the calculations; complex 16, $[Cu(bpy)_2(HCO_2)]BF_4 \cdot {}^1/_2H_2O$, was also excluded because of the possible influence that the hydrogen-bonding water molecule has on the structure of the CuN_4O_2 chromophore. Notice that the line nearly hits the origin (vertical intercept = 0.07 Å).

ellipsoids are small and nearly isotropic for the very asymmetric $[Cu(bpy)_2(CH_3CO_2)]BF_4$ and $[Cu(phen)_2(CH_3CO_2)]BF_4$ complexes but large and very anisotropic for the symmetric $[Cu(phen)_2(CH_3CO_2)]ClO_4$ and $ClO_4 \cdot 2H_2O$ complexes. Also, the angles between the major axes of the O ellipsoids and the Cu–O bond vectors, γ_3, decrease as the acetato group coordinates more symmetrically to Cu(II). These trends are reflected by the rms vibrational amplitudes along the Cu–O bonds, $\Delta U^{1/2}(Cu-O)$, listed in Table V. (These magnitudes are lower than expected for the "symmetric" $[Cu(phen)_2(CH_3CO_2)]ClO_4 \cdot 2H_2O$ and $-BF_4 \cdot 2H_2O$ complexes (both crystallize in the space group $P2/c$, $Z = 2$, with the Cu(II) ions lying on crystallographic C_2 axes[32,34]), presumably due to the strong hydrogen bonding between the acetato O atoms and the water molecules.) The trends are similar for the formato and nitrito complexes.

It is our interpretation that these ellipsoids represent the superpositions of two asymmetric structures with relative contributions ranging from 1:1 for the "symmetric" structures (i.e., those with average C_2 symmetries) to approximately 1:0 for the very asymmetric structures. Support for this interpretation is found by the large and very anisotropic O ellipsoids in $[Cu(phen)_2(CH_3CO_2)]BF_4 \cdot 2H_2O$, which is clearly disordered about a crystallographic C_2 axis, and the small and nearly isotropic O ellipsoids in the isostructural, but ordered $[Zn(phen)_2(CH_3CO_2)]BF_4 \cdot 2H_2O$ complex, which has static C_2 symmetry. This strongly suggests that $[CuL_2(OXO)]Y$ complexes cannot have static C_2 symmetries.[10,32]

Adiabatic Potential Energy Surface Model. A Cu(II) complex with D_3 symmetry, such as $[Cu(bpy)_3]^{2+}$, has a ^2E electronic ground state and is susceptible to a Jahn–Teller distortion.[35] If one of the bpy groups is replaced by a chelating OXO^- group, the resulting symmetry is C_2, and the electronic degeneracy is lifted: the ^2E term splits into a ^2A ground state and a ^2B excited state.[5] Nevertheless, a $[Cu(bpy)_2(OXO)]^+$ cation will be unstable with respect to a pseudo-Jahn–Teller distortion if the splitting of the ^2A and ^2B electronic states in the undistorted complex (2Δ) is sufficiently small and the vibronic coupling integral, $\langle \psi(^2A)|(\partial H^e/\partial S_i')_0|\psi(^2B)\rangle$, is nonzero.[36-41]

An adiabatic potential energy surface model for the pseudodegenerate ^2A and ^2B electronic states in these $[CuL_2(OXO)]Y$ systems that is consistent with the aforementioned crystallographic results and with theory[36-42] is shown in Figure 3.[7,8,32,34] The form of the active distortional mode, shown schematically below the energy minima, corresponds with the pattern of distortion described above in [2]. That this is the principal mode of distortion is indicated in Figure 4 by the linear relationship between the differences in the Cu–O_{eq} bond lengths, $\Delta d(Cu-O_{eq})$, and the differences in the Cu–N_{eq} bond lengths, $\Delta d(Cu-N_{eq})$.

According to the model, if the average site symmetry is C_2, as it is for $[Cu(phen)_2(CH_3CO_2)]BF_4 \cdot 2H_2O$[32] (vide infra), the

(34) Fitzgerald, W.; Hathaway, B.; Simmons, C. J. *J. Chem. Soc., Dalton Trans.* **1985**, 141.
(35) Jotham, R. W.; Kettle, S. F. A. *Inorg. Chim. Acta* **1971**, *5*, 183.
(36) Öpik, U.; Pryce, M. H. L. *Proc. Roy. Soc. London Ser. A* **1957**, *238*, 425.
(37) Gazo, J.; Bersuker, I. B.; Garaj, J.; Kabesova, M.; Kohout, J.; Langfelderova, H.; Melnik, M; Serator, M.; Valach, F. *Coord. Chem. Rev.* **1976**, *19*, 253.
(38) Bersuker, I. B. *Coord. Chem. Rev.* **1975**, *14*, 357.
(39) Hochstrasser, R. M.; Marzzacco, C. A. In *Molecular Luminescence*; Lim, E. C., Ed.; W. A. Benjamin: New York, 1969; 631–656; see pp 637–639 in particular.
(40) Fischer, G. *Vibronic Coupling*; Academic Press: New York, 1984; pp 82–85.
(41) Bersuker, I. B. *The Jahn–Teller Effect and Vibronic Interactions in Modern Chemistry*; Plenum Press: New York, 1984; pp 61–69.
(42) Gregory, A. R.; Henneker, W. H.; Siebrand, W.; Zgierski, M. Z. *J. Chem. Phys.* **1976**, *65*, 2071.

ground-state minima are equivalent (solid curve); otherwise, they are nonequivalent (dotted curve) and separated in energy by ΔE. Thus, the observed structures are not only statistical means weighted according to the relative thermal populations of the two conformers, but they are also temperature dependent for $\Delta E > 0$ [3]. The ΔE values are sensitive to variations in crystal-packing forces, as demonstrated by the significant structural differences between "cation-distortion isomers" noted above in [1]. Accordingly, the symmetrically coordinated acetato group in $[Cu(phen)_2(CH_3CO_2)]ClO_4$ has greater apparent thermal motion than the asymmetrically coordinated group in $[Cu(phen)_2(CH_3CO_2)]BF_4$ because the thermal population of minor conformers at each site in the crystal is greater in the ClO_4 complex, where ΔE is less. The trend continues until "apparent" C_2 symmetry is reached ($\Delta E = 0$), then both conformers are equally present, and even larger and more anisotropic Gaussian ellipsoids are observed. This effect is more pronounced for the acetato complexes than for the nitrito complexes because the pseudo-Jahn-Teller radius S_{pjt}, the distance from the ground-state maximum to either of the symmetrically disposed minima, is greater for the acetato complexes. Thus, the differences in the corresponding $Cu-O_{eq}$ bonds between conformers are greater and the observed O ellipsoids are larger and more anisotropic.[43]

According to the symmetry properties of the vibronic coupling integral, $\langle\psi(^2A)|(\partial H^e/\partial S_i')_0|\psi(^2B)\rangle$, vibronic coupling of the ^2A and ^2B electronic states can occur only if the active vibrational mode has b symmetry, in which case *static C_2 symmetry cannot be retained upon distortion.*[7,32,46] That the $[Cu(phen)_2(CH_3CO_2)]BF_4\cdot 2H_2O$ and $-ClO_4\cdot 2H_2O$ complexes do not have static C_2 symmetries, even though the Cu(II) ions lie on crystallographic C_2 axes,[32,34] is strong evidence that vibronic coupling is operative in these complexes and that the symmetry requirements are being obeyed. A fortiori, the marked temperature dependence of the single-crystal ESR spectra of the 10% Cu-doped $[Zn(phen)_2(CH_3CO_2)]Y\cdot 2H_2O$ (Y = BF_4, ClO_4) systems strongly suggests that these "symmetric" complexes are actually interconverting asymmetric structures (a "dynamic pseudo-Jahn-Teller effect," at least at room temperature) associated with two equivalent and thermally accessible energy minima and that they have average, not static, C_2 symmetries.[34,48]

Determination of the Energy Difference (ΔE) between Solid-State Conformers in $[Cu(bpy)_2(ONO)]NO_3$ by X-ray Diffraction. The structural and vibrational differences between $[Cu(bpy)_2(ONO)]NO_3$ and its isostructural and orbitally nondegenerate d^{10} Zn(II) analogue are even further evidence of vibronic coupling in these Cu(II) systems. According to our vibronic coupling model, the structure of $[Cu(bpy)_2(ONO)]NO_3$ is actually a statistical mean weighted according to the relative thermal population of two conformers separated in energy by ΔE. It is possible to derive

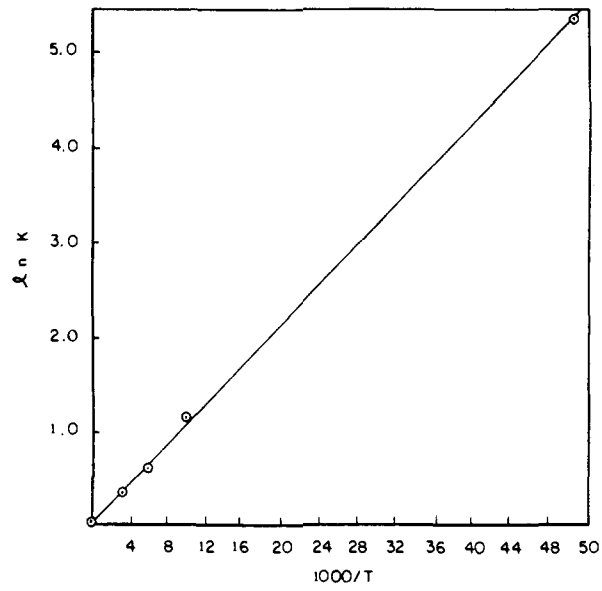

Figure 5. Plot of ln K vs. T^{-1} for S_{pjt} = 0.355 Å (see text).

an equation which relates ΔE to the crystallographically observable S' values

$$S'^2 = \frac{1}{2}\{[\Delta d(Cu - O_{eq})]^2 + [\Delta d(Cu - N_{eq})]^2 + [\Delta d(Cu - N_{ax})]^2\} \quad (2)$$

We envisage that a dynamic equilibrium occurs between all vibronic levels of the two minima. Boltzmann statistics indicates

$$n_r^A = n_r^B \exp(\Delta E/RT) \quad (3)$$

where n_r^A and n_r^B are the relative thermal populations of the vibronic levels of minima "A" and "B", and ΔE is the energy difference between the bottom most vibronic level of minimum "A" and the bottom most level of minimum "B", which is equivalent to the energy difference between the minima. The S' values are weighted according to

$$S' = n_r^A S_{pjt} - n_r^B S_{pjt} \quad (4)$$

where S_{pjt} is the maximum value of S' corresponding to the purely static case. (With this weighting scheme it is implicitly assumed that the degree of distortion from C_2 symmetry is identical for both conformers, i.e., the minima are symmetrically disposed about $S' = 0$, even though they are energetically nonequivalent because of crystal-packing forces.) Inserting eq 4 into eq 3 and rearranging gives

$$\Delta E = RT \ln [(S_{pjt} + S')/(S_{pjt} - S')] = RT \ln K \quad (5)$$

A series of structure determinations at various temperatures, including that at a very low temperature (<20 K), yields S_{pjt} directly and should, in theory, enable ΔE to be determined from a linear least-squares fit of ln K vs. T^{-1}.[49]

The derivation of eq 5 assumes that $n_r^A + n_r^B = 1$, which is true only if the vibronic energy levels above the relative maximum at $S' = 0$ are not populated. Actually, $n_r^A + n_r^B = Z/Z'$, where

$$Z = \sum_i \exp(-E_i/RT)$$

(a summation over the ith levels *below* the energy maximum) and

$$Z' = \sum_i \exp(-E_i/RT) + \sum_j \exp(-E_j/RT)$$

(43) In contrast, the amplitudes and anisotropies of the Gaussian ellipsoids of the ligating atoms in Jahn-Teller CuN_6 and $Cu(N-N)_3$ complexes are significantly smaller by comparison. The reason is simple: the JT radii, R_{jt}, are smaller than the PJT radii because the Cu–N bonds are stronger than $Cu-O_{eq}$ bonds and the force constants correspondingly greater; thus, there is a greater resistance to distortion. (R_{jt} is inversely proportional to the square-root of the force constant.) For example, Ammeter et al.[44] found the R_{jt} values for a series of CuN_6 and $Cu(N-N)_3$ complexes to cluster at 0.32 Å; the pseudo-Jahn-Teller radius for $[Cu(bpy)_2(CH_3CO_2)]BF_4$, however, is ca. 0.59 Å.[45]

(44) Ammeter, J. H.; Bürgi, H. B.; Gamp, E.; Meyer-Sandrin, V.; Jensen, W. P. *Inorg. Chem.* **1979**, *18*, 733.

(45) Hathaway, B.; Ray, N.; Kennedy, D.; O'Brien, N.; Murphy, B. *Acta Crystallogr., Sect. B: Struct. Crystallogr. Cryst. Chem.* **1980**, *B36*, 1371.

(46) Procter et al.[5] report the existence of two vibrationally induced electronic transitions in the polarized single-crystal spectrum of $[Cu(bpy)_2(ONO)]NO_3$. Vibronic selection rules, assuming an effective electronic symmetry of C_{2v} (neglecting the chelate rings, i.e., a *cis*-CuN_4O_2 chromophore), indicate that both transitions activate a vibrational mode of b_2 symmetry.[5] Although a *cis*-CuN_4O_2 chromophore has four b_2 normal modes ($\Gamma_{vib} = 6a_1 + 2a_2 + 3b_1 + 4b_2$),[47] only one corresponds exactly to the distortion pattern described in [2]. This further supports the vibronic coupling model and the mode of distortion in these systems.

(47) Blyholder, B.; Ford, N. *J. Phys. Chem.* **1964**, *68*, 1496.

(48) Clifford, F.; Counihan, E.; Fitzgerald, W.; Seff, K.; Simmons, C.; Tyagi, S.; Hathaway, B. *J. Chem. Soc., Chem. Commun.* **1982**, 196.

(49) The energy difference between the two lowest energy minima (δ_{12}) of the Warped Mexican Hat potential energy surface for a Cu^{2+} doped zinc Tutton salt was determined by using ESR bandwidth data with the following equation identical in form with eq 5[50]

$$\delta_{12} = RT \ln \{[0.27 + (g_1 - g_2)]/[0.27 - (g_1 - g_2)]\} = RT \ln K$$

The maximum difference between $(g_1 - g_2)$, 0.27, was obtained at 8 K; it is analogous to S_{pjt}.

(includes a summation over the jth levels *above* the energy maximum). The correct expression for eq 5 is therefore

$$\Delta E = RT \ln \{(S_{pjt}Z + S'Z')/[S_{pjt}(2Z' - Z) - S'Z']\} = RT \ln K \quad (5')$$

Tentative results indicate that the energy of the active PJT vibrational mode in $[Cu(bpy)_2(ONO)]NO_3$ is ca. 550 cm^{-1}. Assuming that ΔE = 77 cm^{-1} and that no other vibronic levels are below the maximum, $n_r^A + n_r^B$ = 1.000 (20 K), 1.000 (100 K), 0.995 (165 K), and 0.963 (296 K), which suggests that little error is introduced by the original assumption.

To test our model, X-ray data for $[Cu(bpy)_2(ONO)]NO_3$ were obtained at 20, 100, 165, and 296 K, and the structural results are given in Table III. Because data were collected at 20 K and not at absolute zero, $S_{pjt} \neq S'$(20 K), and an algorithm slightly different than the one just discussed was needed to determine ΔE. The method chosen was to make several calculations of the thermodynamic equilibrium constant K by using a series of trial S_{pjt} values, starting with a number slightly larger than the one at S'(20 K), 0.352 Å. A least-squares line was then fitted to the $\ln K_{calcd}$ vs. T^{-1} data for each trial value: that value that corresponds to the best line with a $\ln K_{calcd}$ intercept closest to zero, as required by the model (as $T \to \infty$, $K \to 1$, and $\ln K \to 0$), is S_{pjt}, and ΔE is proportional to the slope. These calculations have been performed, and the results are S_{pjt} = 0.355 Å and ΔE = 77 cm^{-1} (or 220 cal mol^{-1}).[51] A plot of ln K vs. T^{-1} is shown in Figure 5; correlation coefficient ≈0.99.

Ammeter et al.[44] have shown that it is possible to estimate the Jahn-Teller radius of a dynamically disordered complex by analyzing the anisotropic Gaussian displacement parameters of the metal and ligand atoms of this complex and that of an orbitally nondegenerate metal complex in an isomorphous crystal. Accordingly, the mean-square vibrational amplitudes along the directions of the copper-ligand bonds in $[Cu(bpy)_2(ONO)]NO_3$, $U(L_i)$-$U(Cu)$ = $\Delta U(Cu\text{-}L_i)$, are composed of contributions from all PJT active and inactive Cu-L_i stretching vibrations. By subtracting the corresponding amplitudes in $[Zn(bpy)_2(ONO)]NO_3$, $U(L_i) - U(Zn) = \Delta U(Zn\text{-}L_i)$, the contributions from the inactive vibrations are eliminated. Equations 6 and 7 can then be used to estimate S_{pjt}

$$S_{pjt} = [\sum_{i=1}^{6} \langle \Delta d_i^2 \rangle_{pjt}]^{1/2} \quad (6)$$

where

$$\langle \Delta d_i^2 \rangle_{pjt} = \Delta U(Cu\text{-}L_i) - \Delta U(Zn\text{-}L_i) = [U(L_i) - U(Cu)] - [U(L_i) - U(Zn)] \quad (7)$$

Using the room temperature data for $[Cu(bpy)_2(ONO)]NO_3$ and $[Zn(bpy)_2(ONO)]NO_3$, the calculated value of S_{pjt} is 0.346 Å, low by only 3%.[52] The only individual Cu-L_i distortion amplitudes, $\langle \Delta d_i^2 \rangle_{pjt}$, which are nonzero are $\langle \Delta d^2[Cu(1)\text{-}O(27)] \rangle$, 0.060, and $\langle \Delta d^2[Cu(1)\text{-}O(26)] \rangle$, 0.060 Å^2. This is consistent with the montage of ORTEP drawings in Figure 2: because the Cu-O_{eq} bonds are weaker than the Cu-N bonds, $\Delta d(Cu\text{-}O_{eq}) \gg \Delta d(Cu\text{-}N_{eq})$, $\Delta d(Cu\text{-}N_{ax})$, and the disorder is manifested by the large anisotropic Gaussian ellipsoids of the O atoms. Actually, S_{pjt} can be estimated by using only the $\Delta d(Cu\text{-}O_{eq})$ component (at 0 K), i.e.

$$S_{pjt} \approx \frac{1}{\sqrt{2}}[\Delta d(Cu\text{-}O_{eq})] \quad (2')$$

and the value comes out to be ca. 0.345 Å, which is remarkably close to 0.346 Å. Although the Gaussian amplitude tensors obtained from X-ray diffraction are known to contain systematic errors, this and other results[44,55] suggest that such errors are largely eliminated by estimating Cu-L_i distortion amplitudes, which are determined by taking the *difference* between the ΔU's.

Our value of ΔE obtained by X-ray diffraction is comparable to those determined by measuring the temperature dependence of ESR bandwidths for various six-coordinate Cu(II) complexes.[44,57,58] Because the temperature dependence of the structure of $[Cu(bpy)_2(ONO)]NO_3$ obeys Boltzmann statistics, cooperative forces between molecules in the crystal must be extremely weak, which is consistent with the observation that the electronic reflectance and ESR spectra of Cu(II)-doped $[Zn(bpy)_2(ONO)]NO_3$ show no discernible variations from 0.1–100% copper doping.[6,59] In other words, the dominant and localized pseudo-Jahn-Teller active vibrational mode weakly couples with the external (lattice) phonon modes of the crystal. Furthermore, this "cluster" model suggests that the maximum distortion from C_2 symmetry for a given $[CuL_2(OXO)]^+$ cation, as measured by S_{pjt}, is an intrinsic constant, unaltered by variations in ambient forces, such as changing anions. Finally, our results demonstrate that X-ray analysis can provide information about the preferred conformations of molecules and the energy differences between the conformations. This is not generally recognized.[62]

The Possibility of Using X-ray Diffraction to Characterize Adiabatic Potential Energy Surfaces and Relative Ligand Strengths. It can be shown[36-41] that the adiabatic potential energy expression

(50) Silver, B. L.; Getz, D. *J. Chem. Phys.* **1974**, *61*, 638.

(51) Preliminary ΔE values of 155 and 190 cm^{-1} were previously reported;[7-9] they were obtained from iterative calculations by using only the structural results at 165 and 296 K. The value 77 cm^{-1} supersedes these much less accurately determined values.

(52) This methodology assumes that $[Cu(bpy)_2(ONO)]NO_3$ is purely dynamically distorted with an average C_2 axis, which would be true if ΔE = 0. Although ΔE is only 77 cm^{-1}, suggesting that this is nearly correct, the estimated value of S_{pjt}, 0.346 Å, will be slightly low. Nevertheless, S_{pjt} can be better estimated by using the following quadratic regression equation (after Bürgi[53,54])

$$\Delta U(Cu\text{-}O_{eq}) = a + b[\Delta d'(Cu\text{-}O_{eq})] - [\Delta d'(Cu\text{-}O_{eq})]^2 \ (Å^2)$$

where

$$\Delta d'(Cu\text{-}O_{eq}) = \pm\frac{1}{2}\Delta d(Cu\text{-}O_{eq}) \quad \text{[see eq 1]}$$

Using the data for $[Cu(bpy)_2(ONO)]NO_3$ (T = 20, 100, 165, 296 K) and $[Cu(bpy)_2(ONO)]BF_4$ (T = 298 K),[28] a = 0.072 Å^2 and b = 0.023 Å. Thus, the maximum mean-square eigenvalues along the Cu-O_{eq} bonds are 0.072 Å^2 when $\Delta d(Cu\text{-}O_{eq})$ is 0.011 Å, i.e., for a hypothetical purely dynamically distorted $[Cu(bpy)_2(ONO)]NO_3$ complex. Taking $\Delta U(Zn\text{-}O_{eq})$ to be the mean of the two individual U[O(26,27)]-U[Zn(1)] values, 0.010 Å^2, and $\Delta U(Cu\text{-}O_{eq})_{max}$ as 0.072 Å^2, $S_{pjt} \approx (2[\Delta U(Cu\text{-}O_{eq})_{max} - \Delta U(Zn\text{-}O_{eq})])^{1/2}$ = 0.352 Å.

(53) Bürgi, H. B. *Trans. Am. Cryst. Assoc.* **1984**, *20*, 61.

(54) Stebler, M.; Bürgi, H. B., unpublished results.

(55) The values of S_{pjt} determined from the anisotropic Gaussian displacement parameters of the metal and ligand atoms in a purely dynamically distorted $[CuL_2(OXO)]Y$ complex and in the the isostructural Zn analogue appear to be quite accurate. For example, the structures of three different crystals of $[Cu(bipyam)_2(ONO)]NO_3$ and of two different crystals of $[Zn(bipyam)_2(ONO)]NO_3$ (bipyam = 2,2'-bipyridylamine) have been determined recently at room temperature.[56] The crystals are isomorphous and crystallize in the space group *Pccn* with Z = 4. The metal ions lie on crystallographic C_2 axes—the Zn complex has *static* C_2 symmetry; the Cu complex has *average* C_2 symmetry (ΔE = 0). An analysis of the thermal parameters indicates that the values of $\Delta U(Cu\text{-}O_{eq})$, $\Delta U(Cu\text{-}N_{eq})$, and $\Delta U(Cu\text{-}N_{ax})$ obtained for the three Cu crystals are as follows: (1) 0.061, 0.007, 0.002 Å^2; (2) 0.069, 0.007, 0.001 Å^2; and (3) 0.068, 0.008, 0.003 Å^2, while the corresponding values for the two Zn crystals are as follows: (1) 0.010, −0.000, 0.002 Å^2 and (2) 0.008, 0.001, 0.003 Å^2. It is apparent that $\langle \Delta d^2(Cu\text{-}N_{ax}) \rangle \approx 0$. Taking the average values of $\Delta U(Zn\text{-}O_{eq})$ and $\Delta U(Zn\text{-}N_{eq})$ and using eq 6 and 7, the calculated values of S_{pjt} are 0.341, 0.366, and 0.366 Å, respectively, which compare remarkably well (mean = 0.358 Å) with the value determined for the chemically similar $[Cu(bpy)_2(ONO)]NO_3$ complex by using low-temperature X-ray diffraction, 0.355 Å.

(56) Simmons, C. J.; Hathaway, B. J., unpublished results.

(57) Banci, L.; Bencini, A.; Gatteschi, D. *Inorg. Chem.* **1982**, *21*, 1572.

(58) Petrashen, V. E.; Yablokov, Yu. V.; Davidovich, R. L. *Phys. Stat. Sol.* **1980**, *101*, 117.

(59) Repeated attempts to apply Boltzmann statistics to spin-crossover phenomena in the solid state have been unsuccessful because of the large changes in crystal-packing forces which accompany a change in electronic state.[60,61] In contrast, the Boltzmann model is applicable for the $[CuL_2(OXO)]Y$ complexes because there are no changes in electronic states and, as indicated by the unobserved temperature dependence of ΔE, there are no large variations in crystal-packing forces at different temperatures.

(60) Sams, J. R.; Tsin, T. B. *Inorg. Chem.* **1976**, *15*, 1544.

(61) Cotton, F. A.; Wilkinson, G. *Advanced Inorganic Chemistry*; Wiley: New York, 1980; pp 649–650.

(62) Dunitz, J. D. *X-ray Analysis and the Structure of Organic Molecules*; Cornell University Press: Ithaca, New York, 1979; p 312.

for pseudodegenerate electronic states assuming linear vibronic coupling and identical adiabatic force constants for both the ground and the first excited states is given by

$$E_{\pm} = \tfrac{1}{2}kS'^2 \pm \sqrt{(\Delta^2 + a^2S'^2)} \quad (8)$$

$E_{\pm}$ is the energy of the upper (+) and lower (-) energy surfaces, k is the adiabatic or "classical" force constant of the active vibrational mode with symmetry coordinate S', 2Δ is the energy difference between the nondegenerate states of an undistorted molecule, and a is the linear vibronic coupling constant, $\langle\psi_+|(\partial H^e/\partial S_i')_0|\psi_-\rangle$. (Actually, this equation is identical in form with that derived for the effects of first-order spin-orbit coupling on orbitally degenerate states, except that λ, the spin-orbit coupling constant, replaces 2Δ. The removal of electronic degeneracy is then a result of spin-orbit coupling rather than chemical substitution.[63,64]) It is easily shown that if $2\Delta > 2a^2/k$, both curves are parabolas and pseudo-Jahn-Teller distortion does not occur. Otherwise, the lower energy surfaces will have equivalent minima (e.g., for an isolated molecule; see the solid curves in Figure 3) at

$$S_{pjt} = \pm\sqrt{(a^2/k^2 - \Delta^2/a^2)} \quad (9)$$

and distortion from the symmetrical geometry will be spontaneous.

Unfortunately, eq 8 contains three parameters that are extremely difficult to obtain experimentally. Nevertheless, it is possible to derive an equivalent expression of $E_{\pm}$ in terms of parameters that are much more amenable to experimental determination

$$E_{\pm} = (S'/S_{pjt})^2(\sqrt{WB} - B) \pm \tfrac{1}{2}\sqrt{W^2 + (4W/S_{pjt}^2)(S'^2 - S_{pjt}^2)(\sqrt{WB} - B)} \quad (10)$$

W, the transition energy between the ^{2}A ground and ^{2}B first excited electronic state, can be obtained easily from near-infrared visible spectroscopic measurements, B, the barrier height between the ground-state minima, can be obtained from ESR bandwidth experiments,[50] and S_{pjt} can be obtained from very low-temperature X-ray experiments.[65] Three other useful equations follow from this derivation

$$2\Delta = W - 2\sqrt{WB} \quad (11)$$

$$k = (2/S_{pjt}^2)(\sqrt{WB} - B) \quad (12)$$

$$a = S_{pjt}^{-1}\sqrt{W(\sqrt{WB} - B)} \quad (13)$$

For $[Cu(bpy)_2(ONO)]NO_3$, $W = 9620$ cm^{-1} [6] and $S_{pjt} = 0.355$ Å. Assuming a reasonable value of B, say, 500 cm^{-1}, from eq 11-13, $2\Delta = 5230$ cm^{-1}, $k = 26\,900$ cm^{-1} Å^{-2} (or 0.53 mdyn Å^{-1}), and $a = 11\,370$ cm^{-1} Å^{-1}, and are all very reasonable values.[66,67]

For a given series of $[CuL_2(OXO)]Y$ complexes, the values of 2Δ will be proportional to the ligand strengths of the different OXO groups, being zero if OXO is bpy or phen. Attempts to obtain a relative ranking of ligand strengths by measuring the S_{pjt} and B values for a variety of these complexes by using low-temperature X-ray diffraction and ESR techniques are now in progress at the University of Puerto Rico and the University of Iowa.

Acknowledgment. We thank Sten Samson, Richard Marsh, and William Schaefer at the California Institute of Technology and Hans Bürgi, University of Bern, for helpful discussions, the Molecular Structure Corporation, College Station, TX, for their help in obtaining the 165 and 296 K data for $[Cu(bpy)_2(ONO)]NO_3$, and Karl Seff, University of Hawaii, for allowing us to obtain the 295 K data for $[Zn(bpy)_2(ONO)]NO_3$. B.D.S. acknowledges support as a Myron A. Bantrell Research Fellow in Chemical Catalysis at the California Institute of Technology (1980-83) and support for an upgrade of the X-ray Facility by the National Science Foundation (Grant No. CHE8219039).

Supplementary Material Available: Tables of U_{ij}'s (S1, S2, and S3), bond lengths and angles involving hydrogen atoms (S4), and analysis of Gaussian ellipsoids (S5) (13 pages); listing of observed and calculated structure factors (S6, S7, S8, S9, and S10) (61 pages). Ordering information is given on any current masthead page.

(63) Ballhausen, C. J. *Theor. Chem. Acta* **1965**, *3*, 368.
(64) Bacci, M. *J. Chem. Educ.* **1982**, *59*, 816.
(65) Vibrational zero-point energies have been neglected in eq 10; the experimentally determined energy values of W and B should be incremented accordingly. A reasonable value for the $[CuL_2(OXO)]Y$ systems is ca. 275 cm^{-1}.
(66) Nakamoto, K. *Infrared and Raman Spectra of Inorganic and Coordinated Compounds*; Wiley: New York, 1986; p 229.
(67) Deeth, R. J.; Hitchman, M. A. *Inorg. Chem.* **1986**, *25*, 1225.

Crystal and Molecular Structure of Bis(imidazole)(*meso*-tetraphenylporphinato)iron(III) Chloride. A Classic Molecule Revisited

W. Robert Scheidt,* Sarah R. Osvath, and Young Ja Lee

Contribution from the Department of Chemistry, University of Notre Dame, Notre Dame, Indiana 46556. *Received October 15, 1986*

Abstract: The crystal and molecular structure of the low-spin compound $[Fe(TPP)(HIm)_2]Cl$ has been determined by X-ray diffraction methods. The asymetric unit of structure contains two independent half $[Fe(TPP)(HIm)_2]^+$ ions. Each ion has required inversion symmetry, and the two axial ligand planes within each ion are thus parallel. The two ions have distinctly different orientations of the imidazoles with respect to the porphyrin and give rise to two overlapping EPR signals. The differing orientations of the axial ligands also lead to changes in the rhombicity of the coordination bond parameters, a previously unrecognized effect in low-spin ferric porphyrinates. The differing orientations of the axial ligands appear to result from participation in an extended hydrogen bonding network in the crystalline lattice. Crystal data: space group $P\bar{1}$, $Z = 2$, $a = 13.331$ (2) Å, $b = 17.688$ (3) Å, $c = 11.213$ (2) Å, $\alpha = 107.99$ (1)°, $\beta = 94.70$ (1)°, and $\gamma = 69.68$ (1)° at 292 K.

We have been investigating the effects of, and the control of, specific axial ligand orientations on metalloporphyrin physical properties. Work to date reveals that effects appearing to be describable in terms of axial ligand orientations are significant. A convenient method for describing the precise axial ligand orientation in metalloporphyrins, for planar axial ligands, is to

0002-7863/87/1509-1958$01.50/0